Some factors governing the formation of water droplets in the wake zone of flat plates in air streams

A. Evans

SOME FACTORS GOVERNING THE FORMATION OF WATER DROPLETS IN THE WAKE ZONE OF FLAT PLATES IN AIR STREAMS

by

A. Evans

. . . . . being a thesis presented in candidature for the degree of Master of Science in the University of Durham, 1970.

'Some factors governing the formation of water droplets in the wake zone of flat plates in air streams'.

Summary

This thesis is concerned with an experimental investigation into some of the factors governing the formation of water droplets in the wake zone of flat plates. Some reference is made to the effect these droplets have in causing blade erosion in steam turbines. An apparatus has been developed which enables the aerodynamic stripping action on pools of water formed at the trailing edges of flat plates to be studied. The spectrum of droplet sizes produced in the initial breakup in the trailing edge wake zone was obtained from a high intensity, short duration flash unit incorporated into a camera arrangement. The results obtained for varying plate length and air flow conditions have been presented in terms of the Weber, Reynolds and Mach numbers plus plate size parameters.

1. Overall Problem with Review of Literature

The moisture content of the steam in the last low pressure stages of a condensing steam turbine can be up to 12%. This moisture is present in the form of droplets which have a diameter of less than one micron[1] (1)[2]. Gardiner (1) gives an account of the diffusional process involved in the deposition of a small fraction of this available water onto the stator blading. On deposition these droplets flow over the stator blade surface under the influence of steam drag to the trailing edge. They then form into a mass of water sufficiently large for droplets to be detached under prevailing conditions. Using an introscope arrangement the Central Electricity Board (South Eastern Region) have produced a film showing the local flow of water in the last stage of a 60 M.W. steam turbine. This shows the build up of water along the trailing edge of the stator blades and the generation of large drops in the way described. Christie (2) supports the observations of

1. 1 micron = 10^{-6} metres.
2. The numbers in brackets refer to the list of references appended to this report.

the Central Electricity Board by an independant investigation using the same technique on a 120 M.W. steam turbine. He goes further by suggesting that drops up to 1400 microns diameter were observed shedding from the root region of the stator blades. There does however appear to be a lack of published information on the governing factors in the size of droplets shed from the stator blades in the immediate trailing edge region. Since the droplets produced are formed by fixed blades their formation can be studied in detail in the laboratory. The problem has been simplified even farther by some investigations by the substitution of flat plates for blade profiles. Christie (2) from further photographic observations on the trailing edge wake region of a blade cascade in a wet steam tunnel gives the range of droplet sizes torn from the trailing edge as 350-1600 microns diameter. Water droplets injected into the steam upstream of the working section provided the conditions for pool formation on the blades in the cascade. The droplets, which were seen to form at random time intervals were accelerated within the wake zone to a velocity not exceeding 70 ft/s. His results indicate that a droplet of say 400 microns diameter will have accelerated to approximately 32 ft/s after travelling $\frac{3}{4}$in even though

(1) 'Primary atomization' being the formation of relatively large droplets in the immediate trailing edge region.

(2) 'Secondary atomization' being additional breakup further downstream when the droplets are subject to the main stream flow.

Moore noted that primary atomization begins with the accumulation of water on the blade trailing edge. The beads of water were seen to oscillate in a random manner under the action of the steam flow and as more water was accumulated eventually became unstable. Distortion of the water mass became excessive and the sheets and ligaments of water formed were broken up into a spray of droplets. This spray was shed into the wake region where steam velocities were low and droplets up to 1500 microns diameter were formed. These droplets were then accelerated slowly downstream by the wake flow. He suggests that the position of secondary atomization is dependant on the velocities within the near wake, distortion occuring when the relative velocity creates aerodynamic forces sufficient to cause breakup of the large droplets. He goes on to demonstrate that the droplets formed by secondary atomization are rapidly accelerated by the steam flow. Over the remaining observed distance he found the spectra of droplet sizes to be

constant, no additional breakup taking place. Moore presented his results for three values of steam velocity within the range 925 ft/s to 1240 ft/s. They indicate the distribution of mass with droplet diameter. Using a double exposure photographic technique he found that the mean velocity of the droplets within any limited size range was fairly well defined. These results were however for droplets clear of the wake zone. At the upper velocity condition his results for droplet velocity compared favourably with theoretical work by Law (4). Law calculated the velocities of isolated droplets in uniform gas streams. Smith (5) produced results for a blade cascade and a square edged flat plate in a wet air tunnel. He studied photographically the breakup of the water pool at the trailing edge, by air streams at different velocities. The work of Smith was carried out on plates ½in long and 1/16in thick and he was concerned with the establishment of a non-dimensional relationship involving a weber number based on a maximum droplet size existing in the free stream flow. It appeared that some of Smith's measurements may have been made when the droplets were under the influence of the trailing edge wake zone and indeed this is confirmed by interpolation of Goldsteins theoretical curves for velocity

distribution within the wake (12). Smith's photographic axis was taken 0.35in downstream from the ½in plate trailing edge. Goldstein suggests a theoretical wake decay length for this arrangement in excess of 0.35in. Indeed he quotes a value of 0.603 as the ratio between the centre line wake velocity and the free stream velocity at this point downstream from the trailing edge. Subsequent discussion between the author and Smith has revealed that Smith's observations showed that the air flow over the pool formed on the plate plucked off droplets from the pool surface and into the free stream air flow not in fact allowing them to be dragged onto the trailing edge and into the wake. His droplets were therefore free from the wake influence. This is contrary to the observations of Moore (3). Smith's suggestion that all of his droplets were clear of the wake zone was based on purely visual observations since he did not obtain a photographic record of the fact. The camera axis was in the vertical plane normal to the direction of flow so that although it allowed an accurate droplet count, it could not determine whether or not the droplets were in the band immediately downstream from the trailing edge bounded by the two faces of the plate. The free stream velocity in Smith's case was of the same order as that of

Moore; that is slightly higher than that to be covered by the author and Smith's plates were shorter and had a streamlined leading edge. Lane (6) reported on the critical velocity required to rupture droplets of varying diameters in streams of air. Using electronic flash, stages of the rupture of individual droplets exposed to air streams were identified and interpreted in terms of fluid mechanics. The secondary droplets into which a droplet was broken up were found to be progressively smaller as the velocity of the air stream was increased. Lapple and Shepherd (7) produced curves for droplet acceleration on the assumption that the droplet has the drag coefficient of a rigid sphere. They equated the vectorial sum of the frictional force and the external forces acting on a droplet, to the product of its mass and acceleration. Their results were in close agreement with available experimental data. The drag coefficient of water droplets as a function of Reynolds number have been produced by Soderberg (8). He considered the droplets as perfect spheres free from mutual and external interference. Gardner (1) gives the time required for droplet breakup to occur as $t = 2.8 \left(\frac{\rho w}{\rho}\right)^{\frac{1}{2}} \left(\frac{d}{V}\right)$ where ρw is the droplet density and V the free stream velocity. Then using the

method of Lapple and Shepherd to determine the acceleration of the droplets and hence the time interval he demonstrates that all the droplets will break up well before the leading edge of the rotor row is reached. In his analysis Gardner assumed that the droplet was subjected to the free stream velocity for the whole of its travel. This assumption of neglecting the wake zone is not valid. The droplet for approximately the first inch of its travel will be under the influence of the trailing edge wake. He also quotes a typical value of $\frac{1}{2}$ inch for the distance travelled across the gap, a more realistic figure being about 3 inches. These factors do not alter his main conclusions, but do affect the range of maximum droplet sizes which he quoted to be in the region of the rotor row under various conditions. The variation in maximum droplet diameter with steam density for a constant free stream velocity was between 44 and 485 microns. Gardner replying to communications on his paper emphasized that a general analysis of wake effects on droplet sizes has yet to be obtained experimentally.

The significence of the droplets shed into the trailing edge region is that they ultimately lead to rotor blade erosion damage. The liquid water entering the rotor

blades consists of droplets of two different size ranges. One which probably contains by far the greater weight of water has an upper size limit of about one micron, and the other contains droplets in the range 5 to 800 microns diameter. From introscope observations on an 120 M.W. steam turbine Christie (2) estimated the largest droplet recorded in the vicinity of the rotor blades as 450 microns. The fact that droplets up to 1400 microns diameter were seen to leave the stator blades indicates that the larger ones break up during flight, confirming observations by Moore (3). It is the upper range of droplet sizes which cause erosion damage due to their size and angle of impact with the leading edge of the rotor row (5). As a result of their greater inertia, these large droplets cannot be accelerated to the free stream velocity whilst travelling across the gap between the trailing edge of the stator blades and the leading edge of the rotor row. The velocity diagram for these droplets on reaching the rotor blading is shown in FIG.(1.1). These droplets strike the leading edge of the rotor blades at an angle almost normal to the steam inlet angle, and cause erosion damage as illustrated in plates (1.2) and (1.3).

A large amount of literature has been published by Schlichting (9), Goldstein (10) and Kline (11) on the velocity distribution inside the wake zone downstream from a trailing edge. There appears to be a certain amount of agreement in the derived profiles at relatively large distances downstream, but for a turbulent wake the zone adjacent to the trailing edge remains to a large extent undefined. Goldstein (12) produced theoretical curves for the velocity distribution in the wake region of flat plates, and his results have been supported with experimental work by Fage and Falkner (13). The plates in question, however, were thin with very sharp leading and trailing edges and the flow conditions were laminar. Schlichting (9) states that for flat plates, even when the boundary layer remains laminar as far as the trailing edge the flow in the wake is still generally turbulent since the velocity profiles are extreemly unstable.

A detailed study of literature on the overall problem that has been outlined reveals a need for further investigation into the wake region. The authors work in this thesis therefore investigates and attempts to explain some of the factors governing the size of droplets produced in the immediate wake region of a flat plate. To accomplish this

the stripping action of air flow over a pool of water formed at the trailing edge of flat plates has been studied. A modified version of Smith's (5) technique has been adopted specifically to a study of the wake region. For convenience water was supplied directly to the plate surface in preference to the use of wet vapour. This is justifiable as the mechanism of pool formation is irrelevant to this study except in so far as the flow of water was easy to regulate. Air being a convenient fluid to supply in quantity under varying conditions was used in preference to steam. A high intensity flash technique and camera arrangement were used to determine the droplet sizes produced rather than the adoption of direct sampling methods which disturb the flow pattern. Detailed description of the apparatus is given in the following section.

The results showed the product Re.We. (based on the plate length and free stream conditions) to vary linearly with Ma. $\frac{dt}{L^2}$, where d is the mean droplet diameter[4] produced in the immediate trailing edge wake region. The plate length and thickness are represented by L and t respectively

4. The mean droplet diameter of the spectrum is usually quoted in terms of the Sauter mean diameter (S.M.D.) a derivation of which is given in appendix 1.

and Ma is the free stream Mach number.

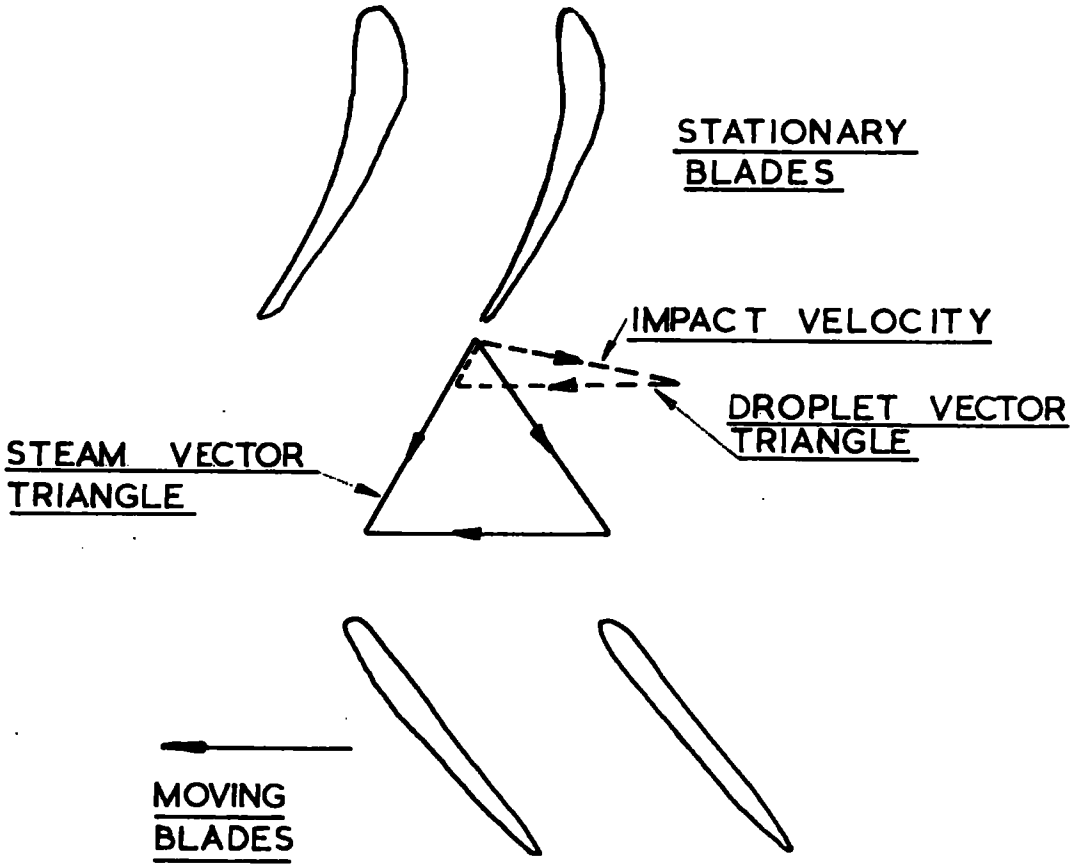

RELATIVE IMPACT VELOCITY OF DROPLETS ONTO MOVING BLADES

FIG. 1.1

STEAM TURBINE ROTOR ROW SHOWING EROSION DAMAGE TO LEADING EDGE

FIG. 1.2

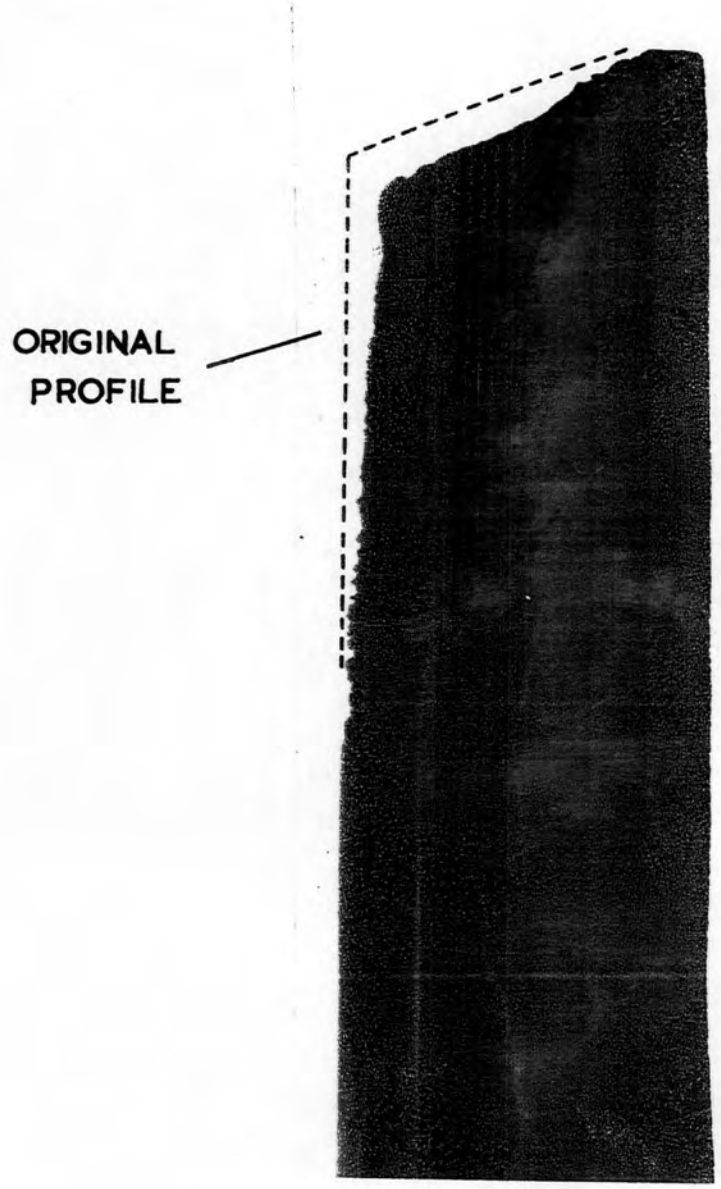

STEAM TURBINE ROTOR BLADE TIP
SECTION SHOWING AREAS OF EROSION DAMAGE

FIG. 1.3

2. Theory

Dimensional Analysis

In order to present the findings of this research programme in the form of independent non dimensional groups a dimensional analysis of the problem was undertaken.

Since we were concerned with the breakup of a pool of water by the stripping action of compressible fluid flow it was assumed that the independent fluid stream parameters of velocity V_ε, density ρ_ε, viscosity μ_ε and bulk modules K_ε should be included. As a measure of the pools resistance to deformation the surface tension σ of water was incorporated. The geometry of the wake region, viscous shear stress and boundary layer thickness over the pool are partially dependent on L the independent plate length. Plate thickness t is also an independent variable upon which the wake geometry will depend, hence the variables L and t were admitted. These seven variables (V_ε, ρ_ε, μ_ε, K_ε, σ, L and t) were considered as the important variables governing the mean size of water droplet initially produced in the immediate wake region of the plate trailing edge. Thus the problem can be represented as $d = f[\rho_\varepsilon, V_\varepsilon, \mu_\varepsilon, K_\varepsilon, \sigma, L, t]$ Use was made of the Π theorem, (proof of which may be found in ref (14).) All the variables may be reduced to the prime

concepts of mass M, length L, and time T and choosing as the repeating variables ρ_E, V_E and L we obtain

$$\Pi_1 = \frac{\mu_E}{\rho_E V_E L} = \frac{ML^{-1}T^{-1}}{(ML^{-3})^{\alpha_1}(LT^{-1})^{\alpha_2}L^{\alpha_3}}$$

$$1 = \alpha_1$$

$$-1 = -\alpha_2$$

$$-1 = -3\alpha_1 + \alpha_2 + \alpha_3$$

$$\therefore \quad \Pi_1 = \frac{\mu_E}{\rho_E V_E L}$$

this is the Reynolds number R_E based on the free stream conditions and plate length.

$$\Pi_2 = \frac{\sigma}{\rho_E V_E L} = \frac{MT^{-2}}{(ML^{-3})^{\beta_1}(LT^{-1})^{\beta_2}L^{\beta_3}}$$

$$1 = \beta_1$$

$$-2 = -\beta_2$$

$$0 = -3\beta_1 + \beta_2 + \beta_3$$

$$\therefore \quad \Pi_2 = \frac{\sigma}{\rho_E V_E^2 L}$$

this is a form of Weber group based on the free stream conditions, pool surface tension and plate length L. The qualification "form" was added because, strictly speaking, the Weber group usually refers to $\frac{\rho V^2 D}{\sigma}$ where ρV^2 is the

dynamic pressure of a fluid flow and D a characteristic dimension of the liquid surface. In its standard form it therefore represents the ratio of the inertia to surface tension forces. In this investigation, however, it is considered more useful to have the plate length L as the geometric dimension. This is acceptable in as much as we are interested primarily in factors controlling the initial droplet size, and not the pool geometry. Throughout the text, this group has been referred to as the Weber number

$$\Pi_3 = \frac{K_E}{\rho_E V_E L} = \frac{ML^{-1}T^{-2}}{(ML^{-3})^{\gamma_1}(LT^{-1})^{\gamma_2} L^{\gamma_3}}$$

$$1 = \gamma_1$$

$$-2 = -\gamma_2$$

$$-1 = -3\gamma_1 + \gamma_2 + \gamma_3$$

$$\therefore \Pi_3 = \frac{K_E}{\rho_E V_E^2} = \frac{K_E/\rho_E}{V_E^2} = M_a$$

this is the free stream Mach number M_a

$$\Pi_4 = \frac{d}{\rho_E V_E L} = \frac{L}{(ML^{-3})^{d_1}(LT^{-1})^{d_2} L^{d_3}}$$

3. Apparatus and Experimental Procedure

3.1 General Layout

The complete wind tunnel, air supply arrangement is shown diagramatically in FIG. 3.1. The wind tunnel section is illustrated in FIG. 3.2. Air is supplied from a positive displacement blower (housed in a small room) operating on the Rootes principle and driven by a 120 h.p. electric motor. Oil free air delivery is assured by special carbon face seals which effectively isolate the rotor chamber from the parts requiring lubrication. Discharge conditions of the blower are 4,000 ft^3/min. free air at 4.5 p.s.i. Air is discharged from the blower to the wind tunnel through 8 inch diameter ducting, any surplus air being discharged to atmosphere. The tunnel itself comprised a 7 inch diameter horizontal duct 11 ft. long with an abrupt nozzle section at outlet converging to 4 inch diameter over 3 inches, thus ensuring uniform turbulent conditions. Free stream velocities up to 650 ft/s. can be obtained at the nozzle exit.

3.2 Noise Problem

On completion of the blower installation, it was found that an unacceptable noise level was produced. This was a combination of actual mechanical transmissions of noise from the blower itself, plus aerodynamic noise down the wind tunnel, and particularly through the bye-pass line

which leads to the outside of the building and was transmitted to the whole of the building. In order to eliminate the high noise level the blower itself was initially insulated. The insulation comprised of an air gap of approximately 10 inches between the blower and a perforated plate, followed by two layers of fibre glass of different densities. The shrouding was completed by $\frac{1}{8}$ inch metal plate. This step considerably reduced the mechanical noise which had previously been radiated into the laboratory and transmitted along the ducting. Silencers were then fitted to the inlet line where it entered the building and the bye-pass exhaust to atmosphere. These silencers were of simple baffle type construction, the annulus being made of perforated plate packed with fibre glass. Finally an in-line silencer was fitted between the blower outlet and the tunnel section. This comprised of a perforated metal duct inside a solid one, and having the annulus packed with fibre glass. These modifications had the combined effect of reducing the sound level produced to give reasonable working conditions.

3.3 Test Section

The brass plates (FIG. 3.3) on which the pool of water was formed, were secured across the nozzle outlet as illustrated in FIG.(3.4). The plates were provided with a

slightly rounded leading edge to maintain a shock free entry. In order to prevent vibration from the air stream the 6 inch plate was supported additionally at mid span. Water from the mains supply was gravity fed to the plate upper surface through 14G hypodermic tubing. Variations in the water flow rate were allowed for by adjustment of the static head above the plate. The depth of pool formed on the plate surface was obtained from a micrometer arrangement (FIG.3.4) which could be swung out over the pool as required A zero reading on the micrometer was obtained against the plate surface before water pool formation. The micrometer tip was then withdrawn and the water supply valve opened. The micrometer was then wound down until contact was made with the pool. A simple electric circuit was utilized to determine the exact contact of the micrometer tip on to the upper face of the pool. (FIG.3.5).

3.4 Instrumentation and Flow Measurement

All measurements relating to air flow rate were taken at an upstream position 7ft. from nozzle exit where the maximum mach number reached was of the order of 0.13, thus allowing incompressible flow theory to be applied. An accurate assessment of the free stream exit velocity from the nozzle was obtained by equating the flow rates between

the low mach number upstream section and the nozzle exit. The total temperature was recorded at the upstream section on a mercury in glass thermometer. A static pressure wall tapping was differentialled against the pitot reading to give the flow velocity. The readings were recorded on manometers using Tetrabramo Ethane and water as the indicating mediums. The pitot probe was manufactured to British Standard Specifications. In order to obtain the exit velocity a quadratic equation in terms of the exit velocity was obtained, which could be solved for different flow rates (see Appendix 2). A cobra type yaw meter was used to investigate the flow in the nozzle exit and plate wake regions. The sensitive geometry of the probe as illustrated in FIG.3.6 enabled the region adjacent to the plate surface to be investigated. The probe was supported such that movement relative to the plate was possible in any direction, (FIG.3.7). The water flow rate to the plate was determined from the calibrated feed bottle.

3.5 Droplet Sampling Technique

The method adopted in this research project to determine the droplet sizes produced in the immediate wake region is photographic. The required illumination being a very short and intense flash during the period of camera shutter

opening. It was chosen because of its relative simplicity, accuracy and the important factor of not disturbing the flow pattern. There are, however, many alternatives available, these are discussed in Appendix 3. The camera was focussed onto the plate trailing edge and the droplet spectrum produced over the region from the plate trailing edge to approximately 0.75 inches downstream recorded. The photographs were analyzed using a calibrated graticule, which classified the droplets in size bands. Counts of droplet sizes taken from the films were quoted in terms of the Sauter Mean Diameter (see Appendix 1).

3.6 Photographic Arrangement

A high voltage, low capacity power source was developed which gave a decay period of approximately 0.2 micro seconds. Since the droplets were accelerating from rest during this period it was sufficiently short to arrest motion. The electrical voltage multiplier circuit and light source - lens arrangement are shown in figures 3.8 and 3.9 respectively. In the light source three T.C.C. cathodray 0.01 μF capacitors are charged in parallel at high voltage (up to 10KV). The discharge is initiated by applying a positive triggering pulse (up to 5KV) to a third electrode which ionizes the spark gap, thus destroying its ability to

hold off the voltage of the charged capacitors, hence initiating the main discharge. Critical adjustment with the relative electrode spacings was required to prevent misfirings. The process of cumulative breakdown of the main gap after passage of the triggering current was practically instantaneous, and so the problem of synchronising the light source resolved itself into one of synchronising the high voltage trigger pulse. Once initiated the main flash discharged into the cone shaped anode providing a point light source which was transformed into a parallel beam of light by placing two plano-convex lenses of small focal length at its focal length from the discharge. The light source was arranged to direct a parallel beam of light onto the camera lens, hence giving background illumination to the water droplets. The camera consisted of a long, light-tight wooden box mounted in line with the light source on the opposite side of the tunnel. At the back of the box a polaroid 4 x 5 land film holder was mounted in a 4 x 5 graflok back with focusing screen and at the front a Kodak Ektar f203 m.m. f7.7 - f45 lens, the arrangement giving a calculated magnification of six. Both the flash unit and the camera were mounted on a common platform enabling movement in any direction relative to the

tunnel. The photographic arrangement is illustrated in FIG.(3.10). The camera was focussed by providing a continuous light source (behind a marked glass screen) at the axis of the tunnel, and racking the camera until it was in focus (FIG.3.11). The depth of field was found to be $\pm$ 0.5 inches. Polaroid PN 57, 3000 A.S.A. film was chosen, the reason being twofold.

1. The film is very fast and fine grained thus picking up smaller droplets and allowing reasonable clarity under poor lighting conditions.
2. Results are obtained directly therefore allowing immediate modifications to be made resulting in a minimum time wastage. No synchronisation was attempted between camera shutter and flash. The operation was a manual one of opening the camera shutter, initiating the flash and releasing the shutter, (the shutter opening time overlapping the spark discharge interval).

A more detailed account of the electric spark in air is given in Appendix 4.

3.7 Rig Calibration

Calibration of the photographic arrangement to improve the clarity of the photographs involved varying the camera settings, intensity of flash, choise of film and also the

use of coloured water. It was necessary to shroud the tunnel exit working section with a sheet metal hood to reduce any stray light to a minimum. Funnels were placed over both the camera and spark discharge lenses to concentrate the illumination onto the subject. These shrouding modifications are not shown on the illustrations of the apparatus.

The pitot probe was calibrated over the working range of mach number as illustrated in FIG.(3.12).

Velocity traverses were obtained at the upstream tapping position in both planes. To ensure a uniform profile at the nozzle exit velocity traverses in both planes at various positions along the plate were obtained. The 'cobra' type yaw meter gave the angle distribution of the air stream at the nozzle exit. To ensure correct alignment the yaw meter was lined up with a parallel flow source (on tunnel axis pointing up tunnel) and swung through 180°. This method is illustrated in FIG.(3.13).

The air flow rates at the upstream and exit positions were independently calculated. For the upstream position the pitot reading gave the velocity and hence from the temperature reading and tunnel dimensions the flow rate was determined. For the exit condition a velocity traverse was

undertaken with a plate in position. Substituting the effective exit area and temperature enabled computation of the flow rate to be completed and comparison made with that calculated for the upstream position.

Water flow rates and pool depth measurements were noted over the working range of exit velocity for different plate lengths.

3.8 Test Procedure

Before starting a test the plate was checked for correct alignment and zero incidence. The camera was then focussed onto the plate trailing edge axis and the voltage multiplier unit adjusted to obtain the correct spark discharge. On starting the blower the valves were regulated to achieve the correct flow rate. Checks were then made to ensure that the water flow rate, which was kept constant throughout the test programme was correct. The pool depth was then recorded and the air flow parameters noted. The calculations required to determine the flow rate are given in Appendix 2. Photographic recordings of the wake region were obtained by opening the camera shutter manually, initiating the flash and closing the shutter. The film was immediately removed and processed. Three photographs were taken at each air flow setting to ensure consistency of

results. In order to relate the water used in the tests to distilled water, random checks were carried out to determine the surface tension. Samples were analysed over a temperature range. The water was allowed to attain room temperature before being supplied to the plate. Velocity profiles within the plate wake zone were obtained by lining the 'cobra' probe up centrally on the plate axis, traversing downstream and recording the total head at regular distances from the trailing edge. The static pressure in the air stream was assumed atmospheric which is justifiable for the range of mach number covered by the test programme.

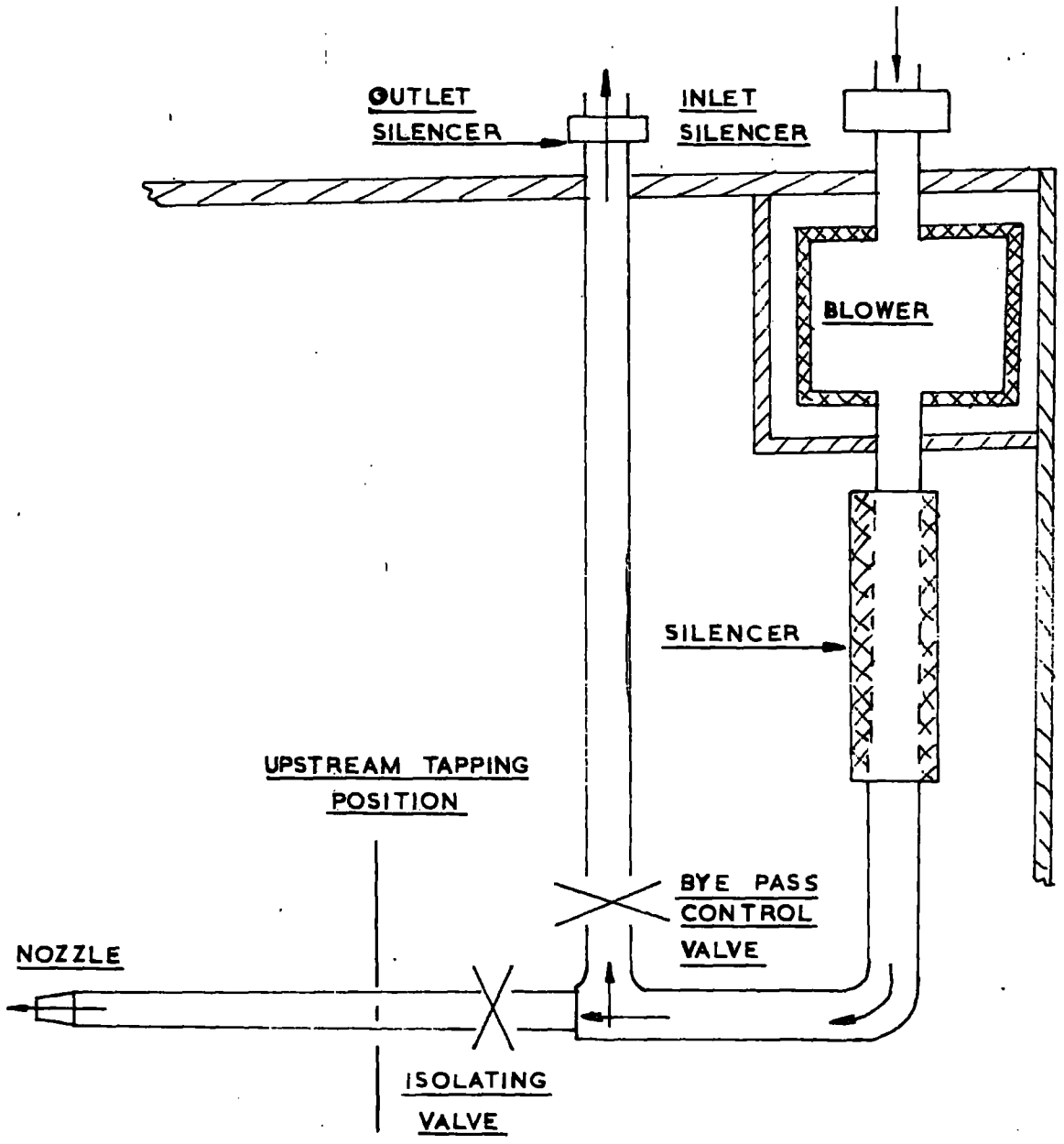

WIND TUNNEL AIR SUPPLY ARRANGEMENT

FIG. 3·1

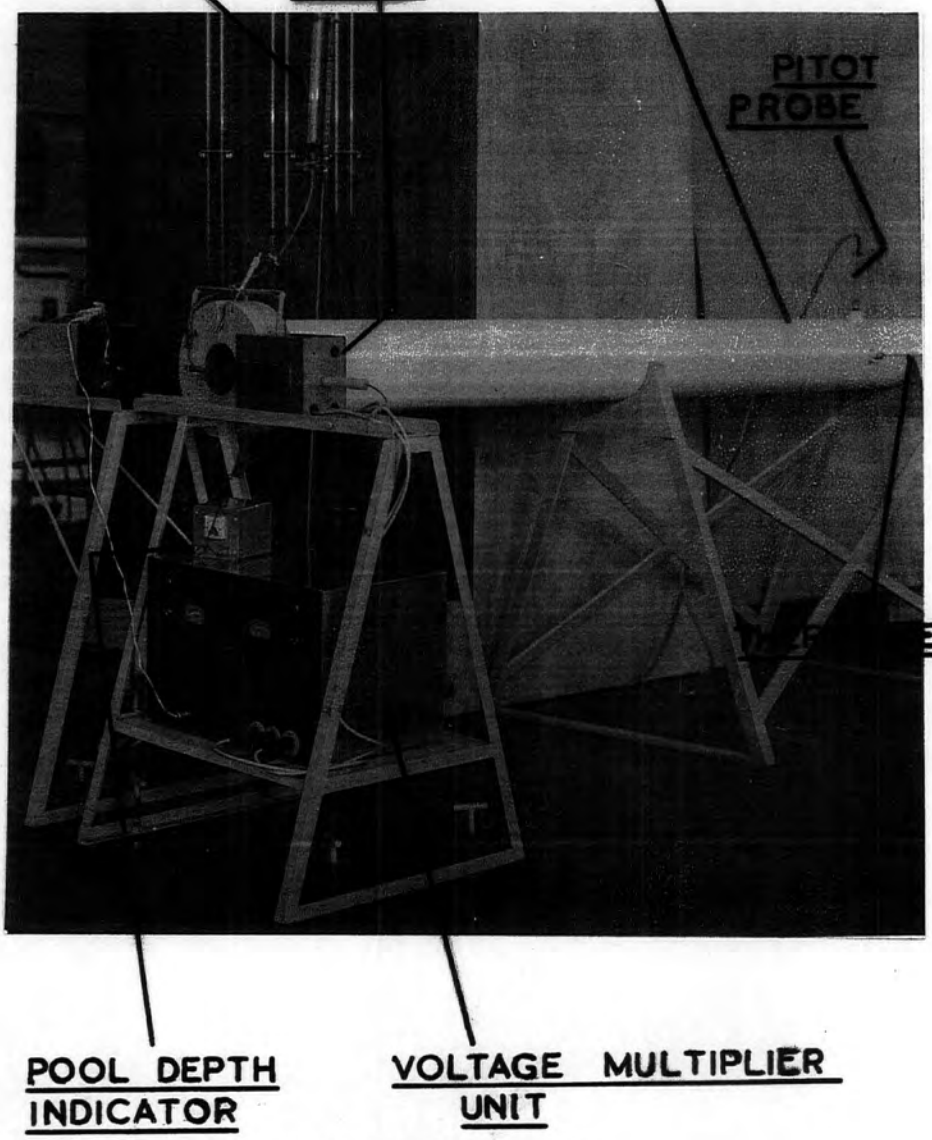

WIND TUNNEL ARRANGEMENT

FIG. 3.2

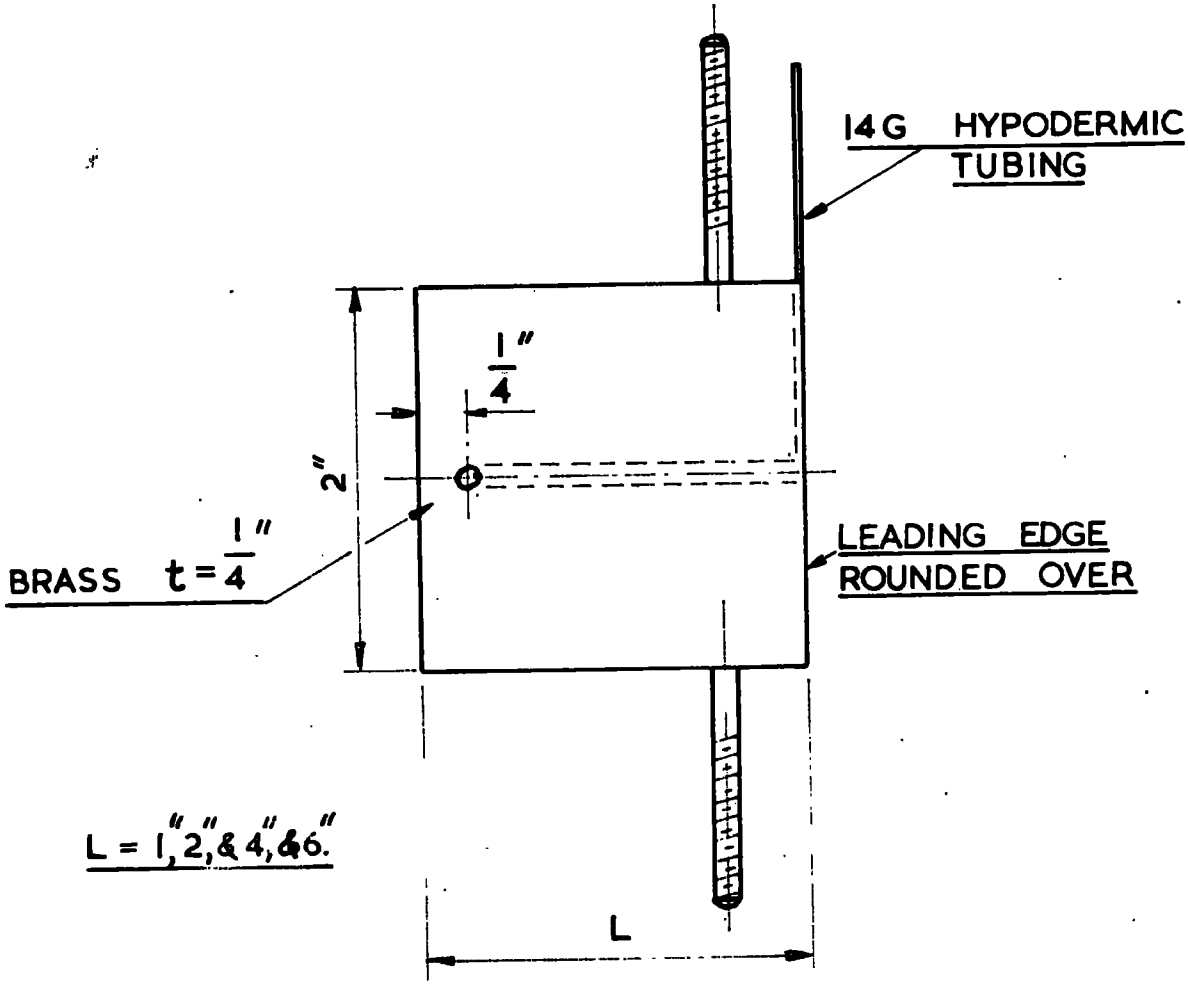

DIMENSIONS OF BRASS PLATES

FIG. 3.3

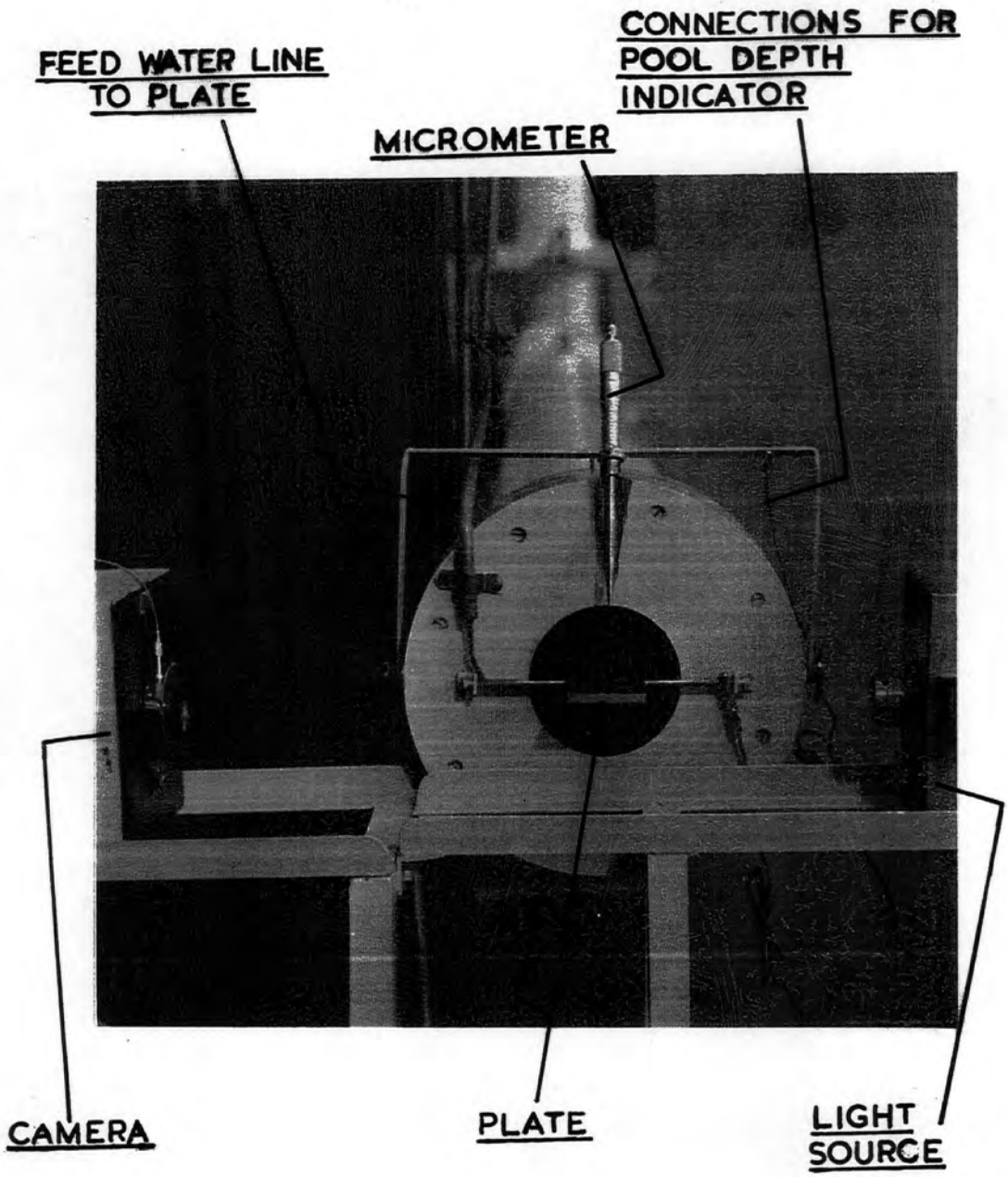

ARRANGEMENT AT NOZZLE OUTLET

FIG. 3.4

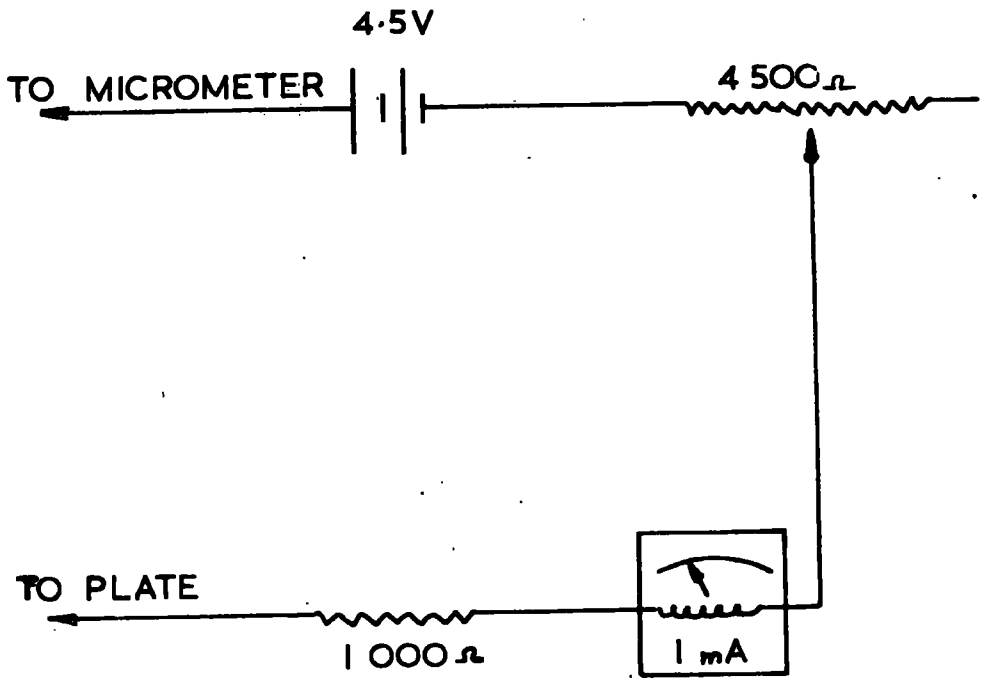

ELECTRIC CIRCUIT UTILIZED
IN POOL DEPTH MEASUREMENT

FIG. 3.5

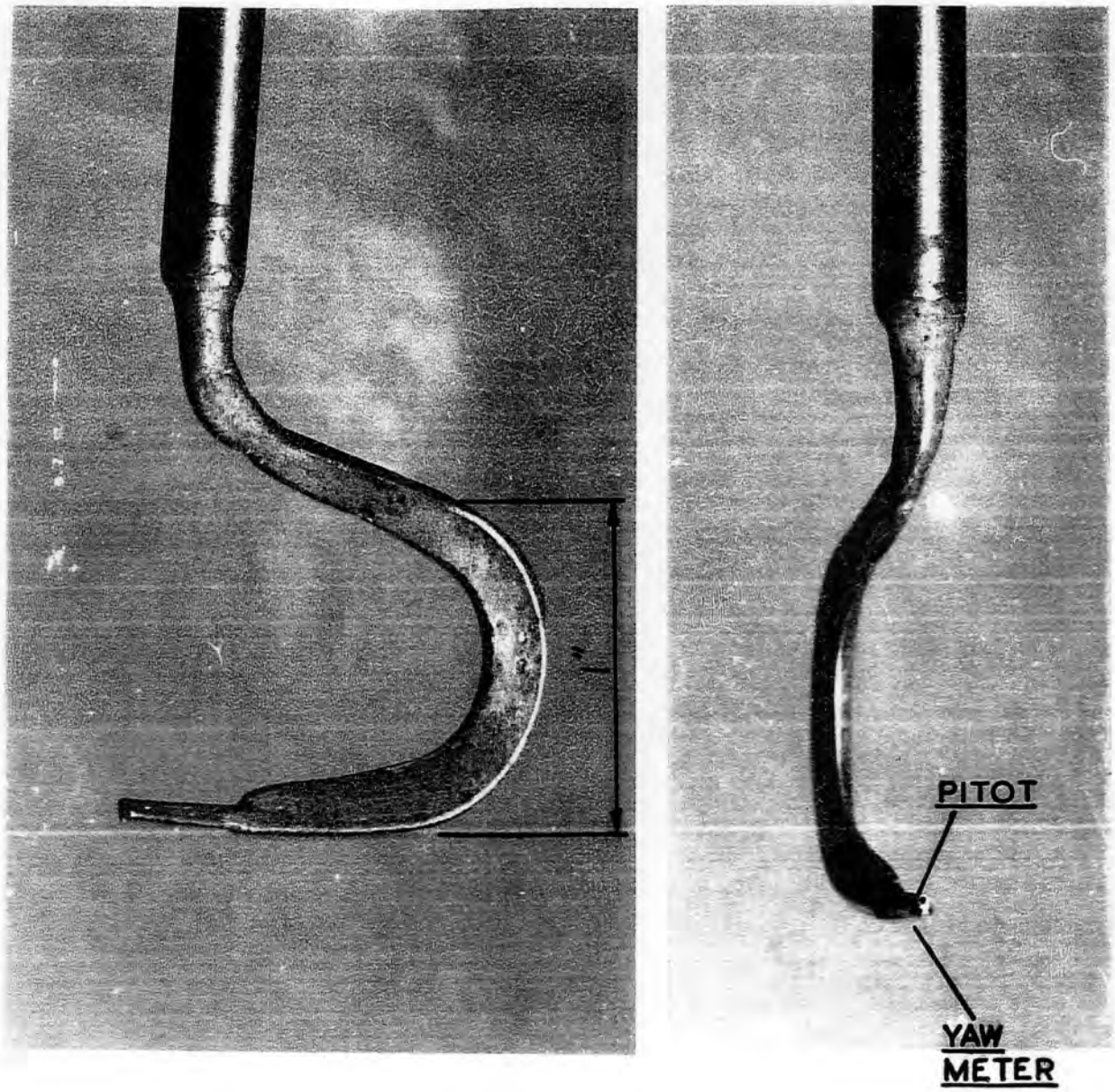

'COBRA PROBE'

FIG.3.6

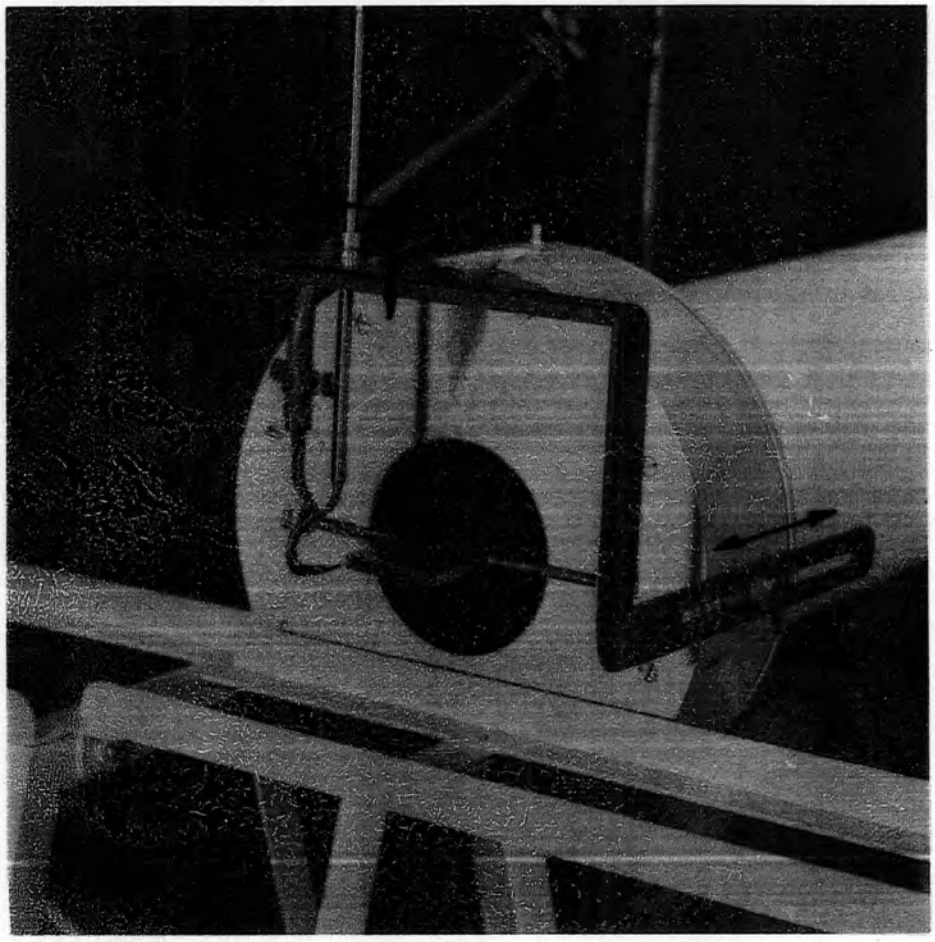

TRAVERSING ARRANGEMENT

FIG. 3.7

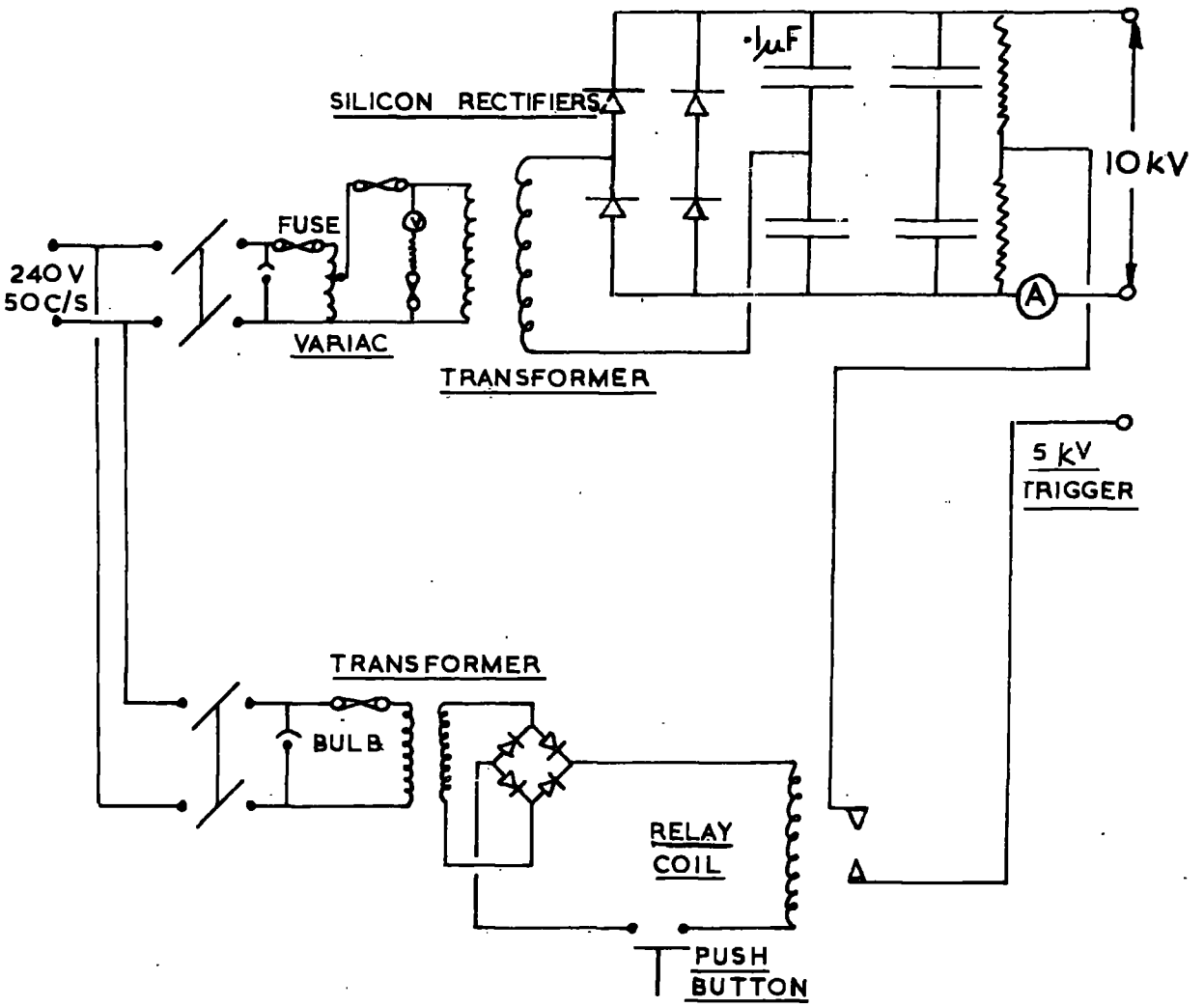

DIAGRAMATIC ARRANGEMENT OF VOLTAGE MULTIPLIER CIRCUIT AND TRIGGER SUPPLY

FIG. 3·8

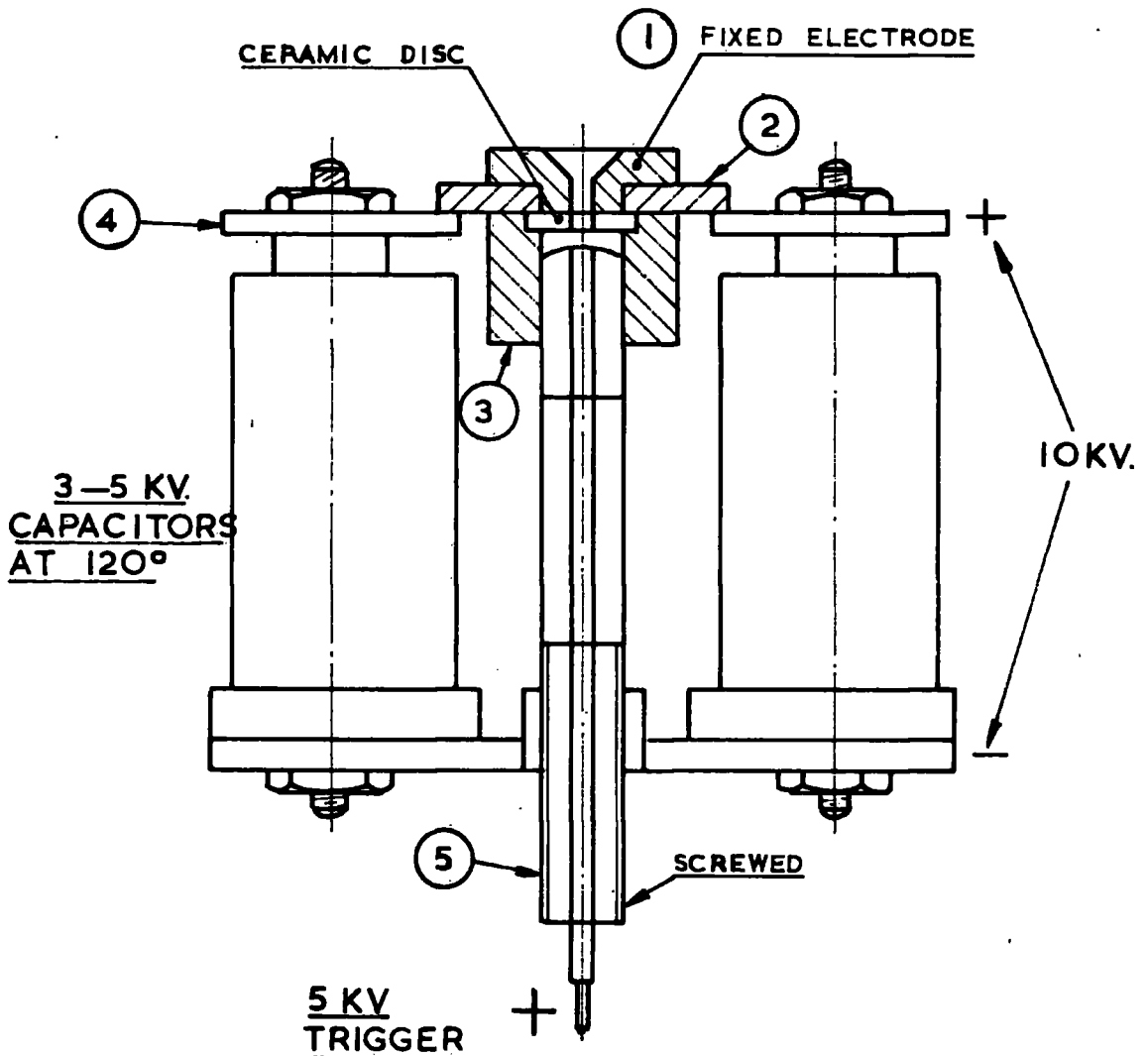

MATERIAL

(1) STAINLESS STEEL
(2)(4) ALUMINIUM
(3) P. T. F. E.
(5) COPPER TUBE – STAINLESS STEEL TIP

LIGHT SOURCE

FIG. 3.9

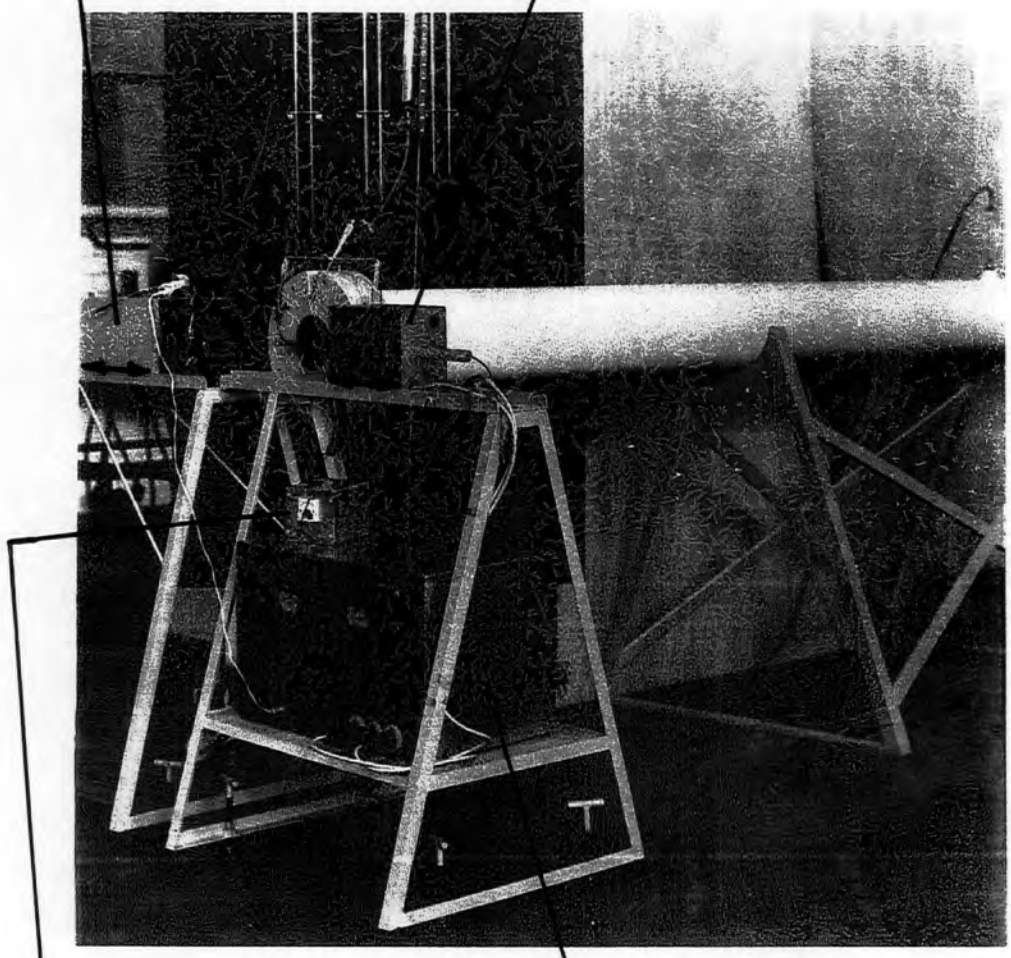

PHOTOGRAPHIC ARRANGEMENT.

FIG. 3.10

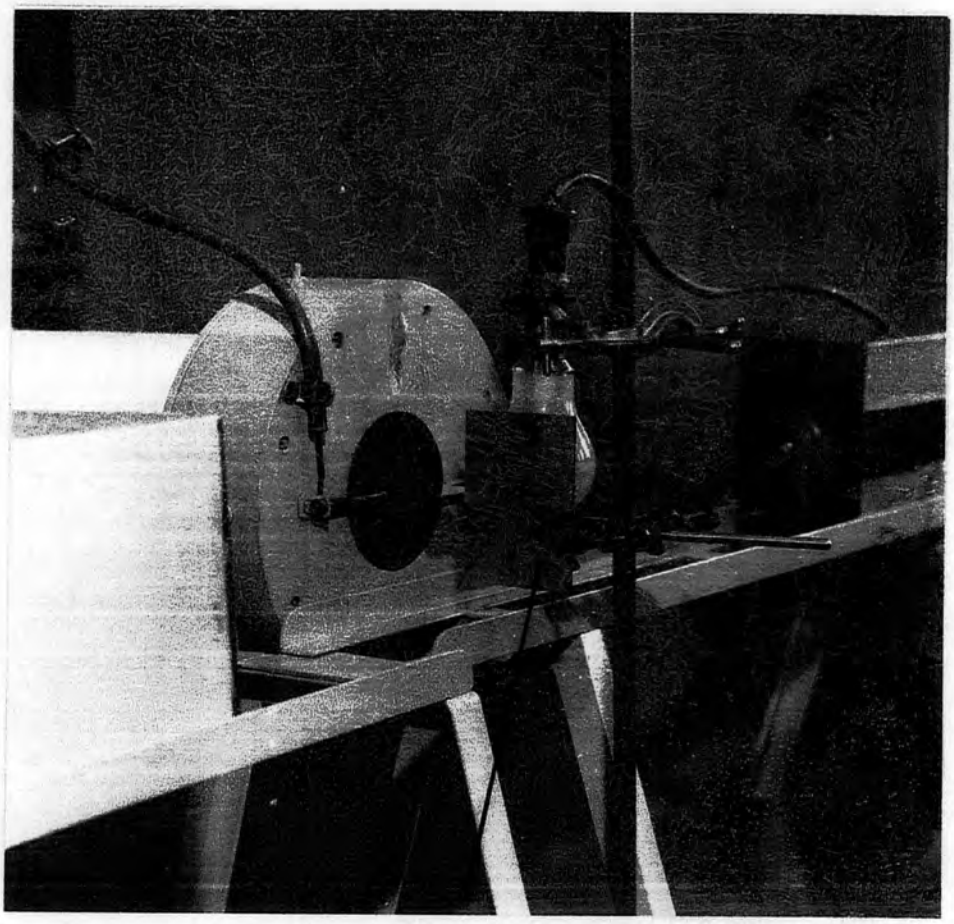

CAMERA FOCUSSED ON PLATE WHICH WAS LINED UP WITH DROPLET TRAJECTORY

FOCUSSING ARRANGEMENT

FIG. 3.11

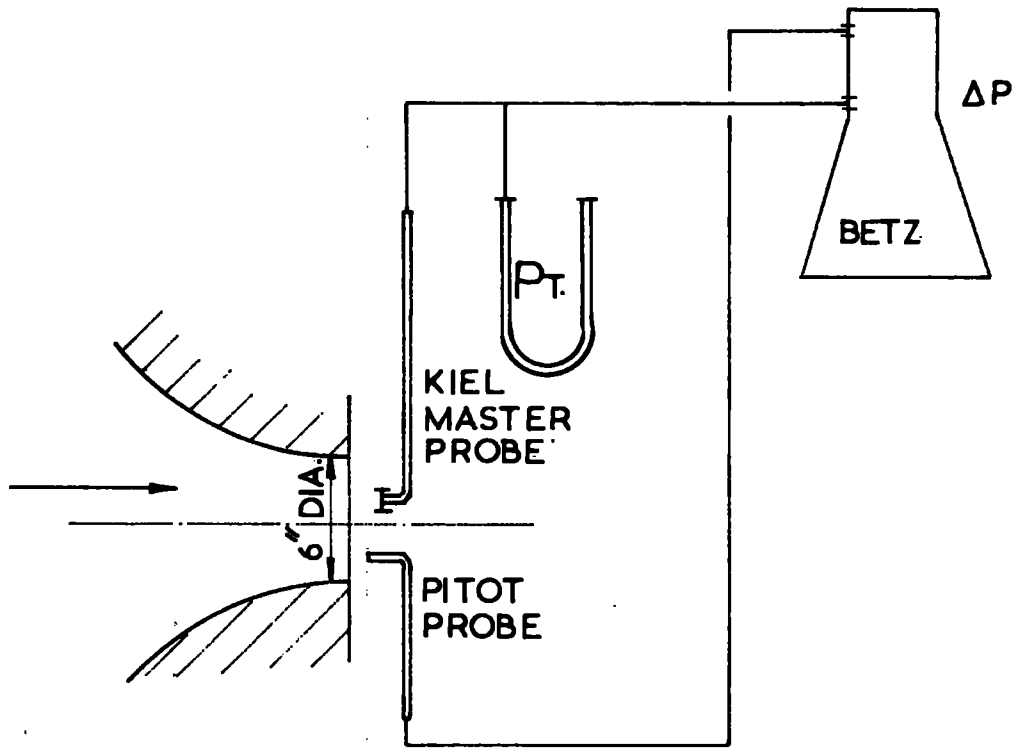

CALIBRATION OF PITOT PROBE

FIG. 3.12

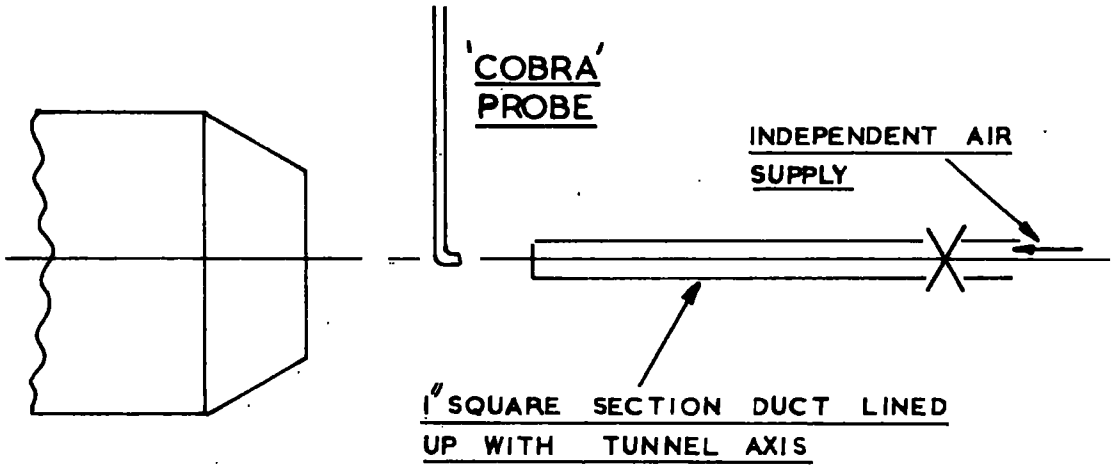

AFTER ADJUSTING THE PROBE FOR ZERO YAW WITH THE PARALLEL SOURCE IT WAS TURNED THROUGH 180° TO BE IN LINE WITH THE TUNNEL AXIS.

METHOD OF PROBE ALIGNMENT

FIG. 3.13

4. Observations and Derivation of Results

4.1 Rig Calibration

The results of the pitot probe calibration are given in FIG.4.1. The probe read true total head up to at least 0.5 mach number and accepted a minimum of $\pm 10^{\circ}$ pitch and yaw. Results of the velocity traverse at the upstream position are given in FIG.4.2. The profile is fully turbulent and it was found that the pitot reading recorded at the centre of the tunnel cross section was of the same magnitude as the integrated mean taken from FIG.4.2. The slight increase in velocity head at the bottom of the curve due to the flow around the bend has been accounted for by the boundary layer thickness. Velocity profiles at nozzle exit are shown in FIG.4.3 for both horizontal and vertical traverses. A uniform turbulent profile was found to exist well beyond the nozzle exit confirming the findings of Taylor (15). The effect of plate disturbance on the exit conditions was determined from a horizontal total head traverse $\frac{1}{4}$ inch above the 2 inch plate surface, $\frac{3}{4}$ inch from its leading edge. The maximum yaw angle was found to be $\pm 5^{\circ}$ and reference to FIG.4.4 shows that a uniform profile over the plate width of 2 inches was obtained. An independent determination of flow rates gave 3.04 lb/s and

2.99 lb/s for the nozzle exit and upstream positions respectively. For the exit condition a velocity traverse was obtained $\frac{3}{4}$in. from the leading edge of the 2 inch plate, 1/16in. above the surface, the mean velocity being determined from the resulting plot. These results are shown in appendix 5. It was found that variation in the nozzle exit air velocity had no effect on the water flow rate, or indeed on the pool depth formed on the plate upper surface. The assumption of taking the static pressure of the exit air stream as atmospheric was confirmed by using the hypodermic feed water line to the plate surface as a pressure tapping and obtaining a series of readings from it relative to the atmosphere. The maximum deviation was found to be $\pm$ 0.5 in W.G.

4.2 Test Results

It was established by a total head traverse in the downstream direction on the plate axis that the wake decay length was greater than 1 inch for the complete flow range over various plate lengths. Since the camera lens was set to cover the area from the plate trailing edge to a point $\frac{3}{4}$ inch downstream, then all the sizes recorded were for droplets under the influence of the immediate wake region. Figure 4.5 shows a typical photographic recording with a

magnification of six. Random samples of the mains water which was supplied to the plates and distilled water were analized, the results showing that the difference in surface tension between the two samples was negligible. The variations in surface tension values with water temperature were allowed for in the results.

It was observed that the pool formed on the plate upper surface was pulled around the trailing edge where it tended to 'drool' along the entire trailing edge face before being plucked off in a seemingly random fashion. All the droplets were contained within a narrow band. Reference to figure 4.5 shows this band to be within the plate thickness viewing from the side across the droplet trajectory. Looking down on top of the plate revealed the droplets to be in a narrow band after a very short distance from the trailing edge had been achieved. Photographs taken over the lower velocity flow range showed a relatively small number of irregular shaped droplets. These droplets which were seen to break up into smaller spherical droplets as the flow progressed downstream were neglected in the analysis. The tables of results in appendix 6 show the photographic recordings for the four plate lengths and the air flow parameters relating to each photograph. These tables indicate the size range and number

of droplets recorded. It is seen that the largest droplet recorded is in the region of 600 microns, and that these were recorded in the wake zone of the 6 inch plate for the lower velocity tests. This is as one would expect, the longer plate producing a slightly longer wake (for a given velocity) and the smaller free stream velocities producing a low velocity within the wake itself. It is seen also that the number of droplets recorded in the lower velocity range is less than that for the higher range, this becoming more apparent with increase in plate length. The histogram shown on FIG.4.6 indicates the variation in number of droplets recorded with size for two velocities. The scatter in the calculated S.M.D. for the three photographs taken at each test condition is seen to be much greater over the lower velocity range. However, from comparison of the three photographic counts it is seen that a reasonable consistency was obtained.

The results of the velocity traverse in the wake region are shown in FIG.4.7. Throughout the test programme the water flow rate to the plate was kept constant at $0.246.10^{-2}$ lb/s. Pool depth measurements gave a constant reading of 0.005 inches ($\pm$ 0.001) over the air flow range. The reduction of droplet size due to evaporation (1) is only of

the order of 1.10^{-5} microns on a 100 micron diameter particle and has thus been neglected. Dimensional analysis of the parameters affecting the droplet size produced in the immediate trailing edge wake region gave the Reynolds, Weber and Mach numbers, and the groups $^{d}/_{L}$ and $^{t}/_{L}$ as the important non-dimensional groupings. The results were therefore presented in terms of such groups and are tabulated in appendix 6, and illustrated graphically in FIGS. 4.8 and 4.9. In figure 4.9 the curves for the four plate lengths tested were brought together onto a single curve by plotting Ma. $^{d}/_{t}$ against the product Re. We. It could be argued, however, that the only true experimental variables in the five non-dimensional groupings were the droplet mean diameter d, the free stream velocity V_E and plate length L. The remaining parameters if not in fact constant throughout the test programme, varied only by insignificant amounts certainly not sufficient to form definite trends. The majority of the remaining parameters were functions of exit air temperature which had a maximum variation of $36.7^{\circ}F$ in the test programme. Further plots were therefore obtained involving the true experimental variables. Figure 4.10 shows the variation of d with V_E for each plate length to be a straight line relationship. The plot of d against the effective

variables in the Reynolds number $V_E X.L$ for each plate (figure 4.11) also results in a linear relationship. The effective variables in the Weber number are plotted as the product $V_E{}^2 L$ with d in figure 4.12 for each plate length the form of which is curvilinear.

Kiel 'Master' Probe "W.G.	$\frac{\Delta P}{\text{Master Pitot}}$ "W.G.
7.6	0
14.0	0
22.5	0
32.4	0
44.0	0
51.5	0
58.2	0
60.0	0

BARO = 30.08 "Hg @ 65°F

At maximum flow

Ma = 0.45

The probe accepts a minimum of $\pm$ 10° pitch and yaw without registering any deviation from the master reading.

CALIBRATION OF PITOT PROBE

FIG. 4.1

UPSTREAM VELOCITY TRAVERSE

VERTICAL TRAVERSE FROM TOP

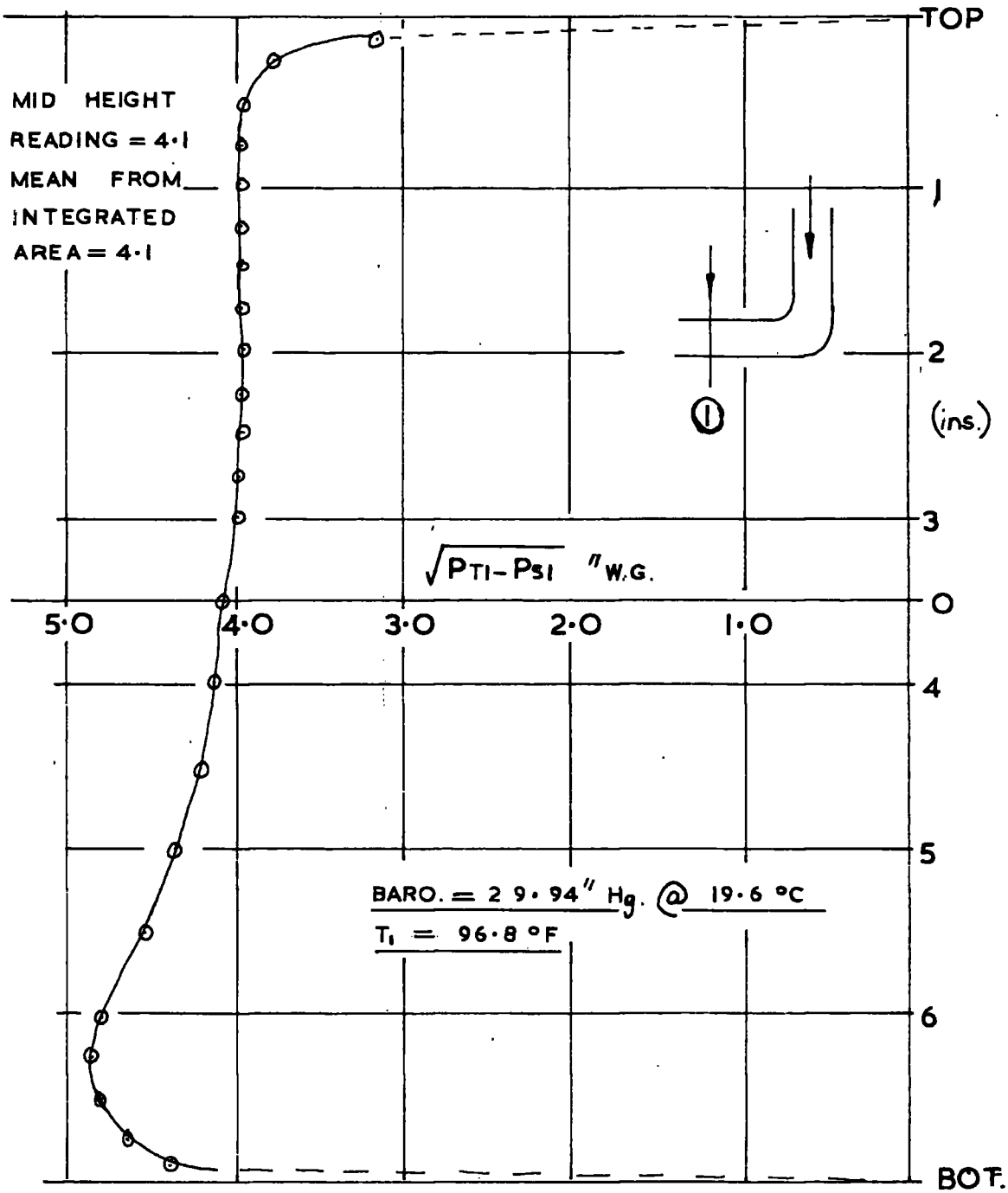

FIG. 4·2

TOTAL HEAD TRAVERSE AT NOZZLE EXIT

ON DIAMETER 1¼" FROM NOZZLE EXIT (PLATE REMOVED)

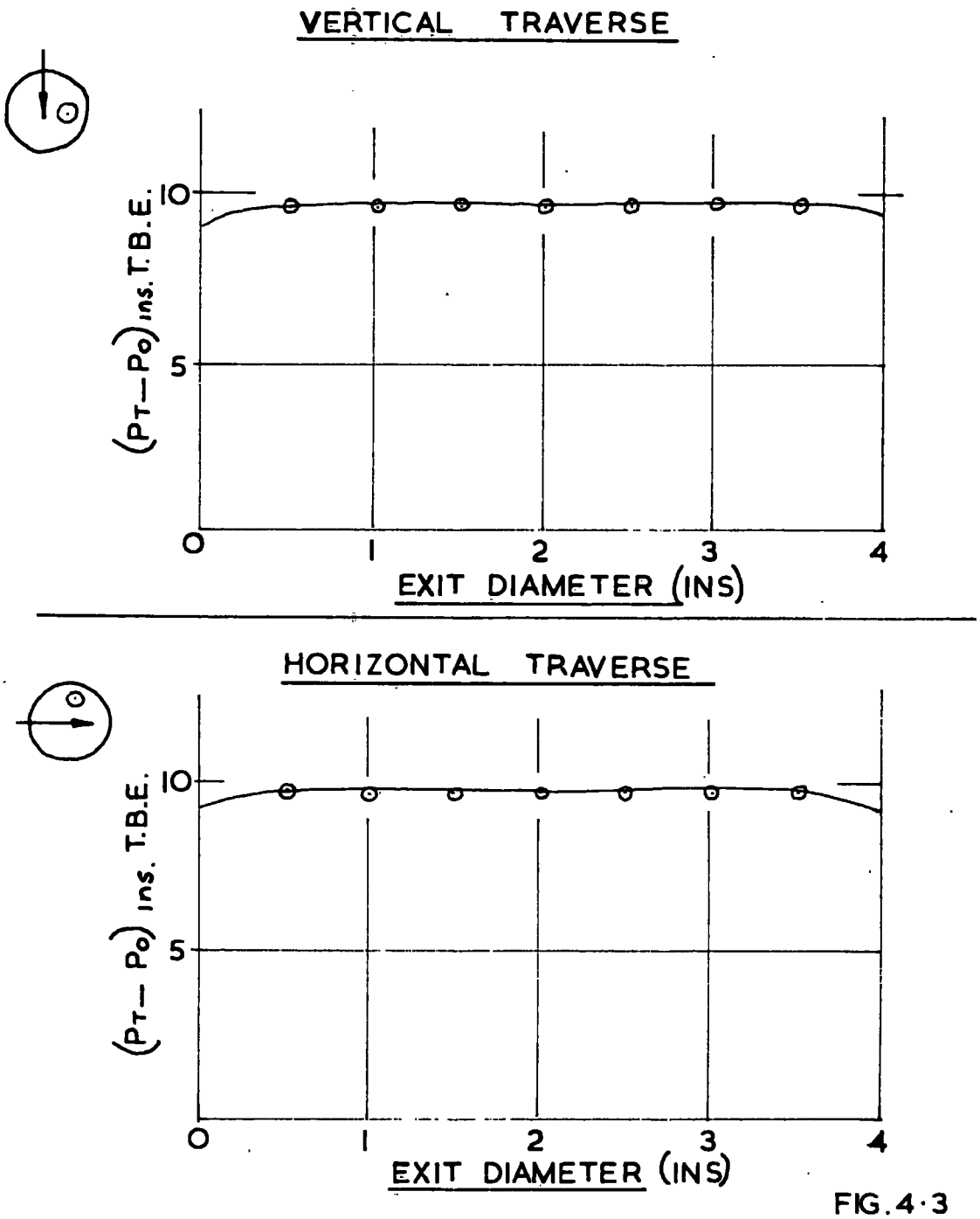

FIG. 4·3

TOTAL HEAD TRAVERSE $\frac{1}{4}$" ABOVE 2" PLATE $\frac{3}{4}$" FROM L.E.

MAX. YAW ANGLE RECORDED = ± 5°

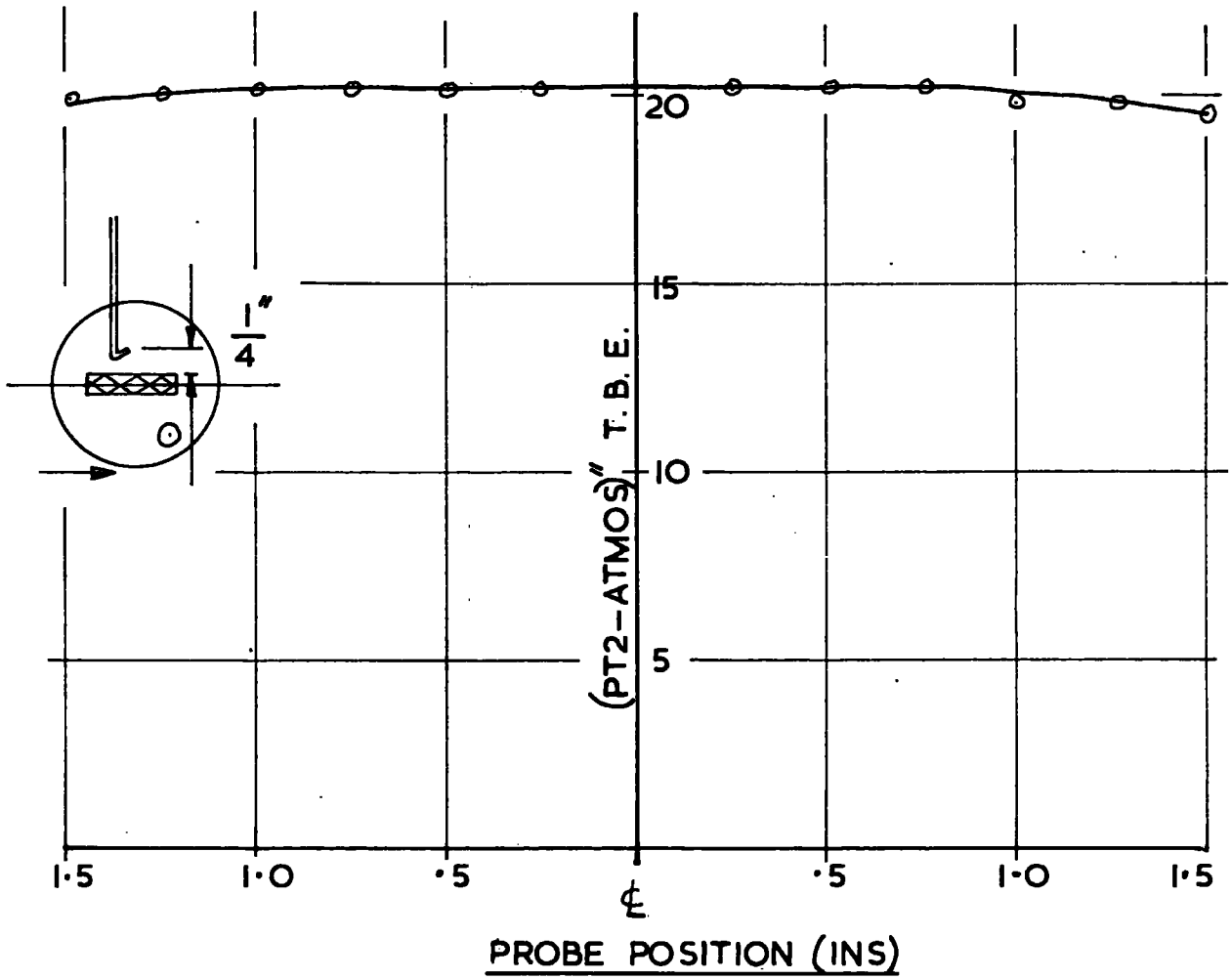

FIG. 4·4

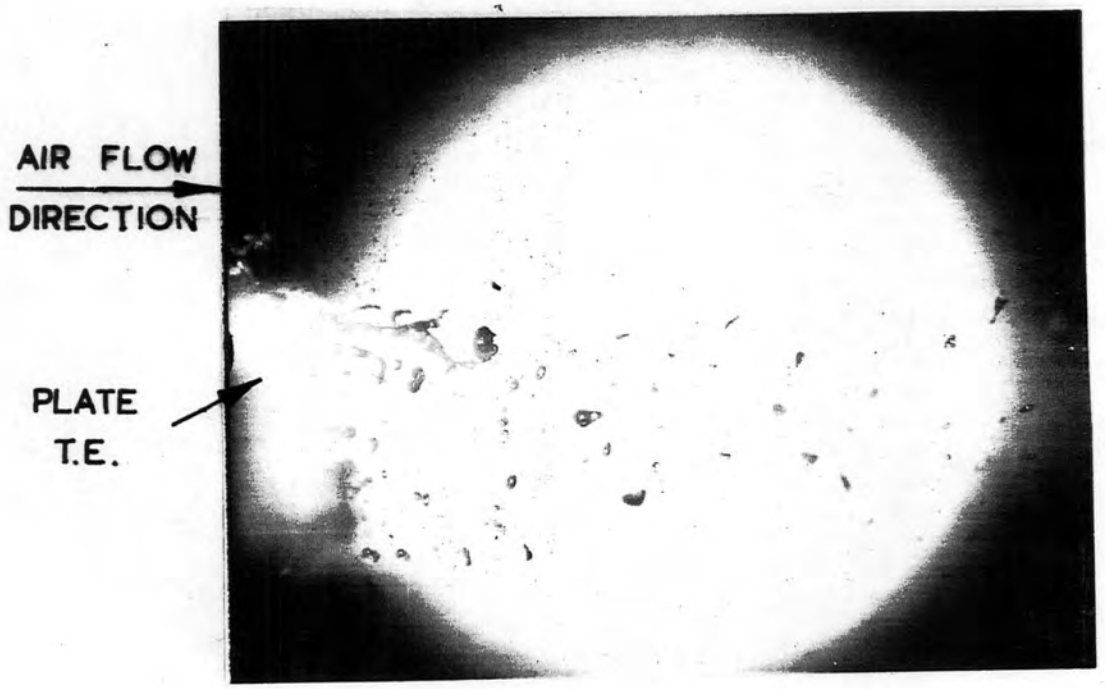

PLATE LENGTH = 6"
AIR VELOCITY = V_E = 305 FT/s

DROPLET SPECTRUM IN TRAILING EDGE
WAKE REGION

FIG. 4.5

VARIATION IN NUMBER OF DROPLETS RECORDED WITH SIZE

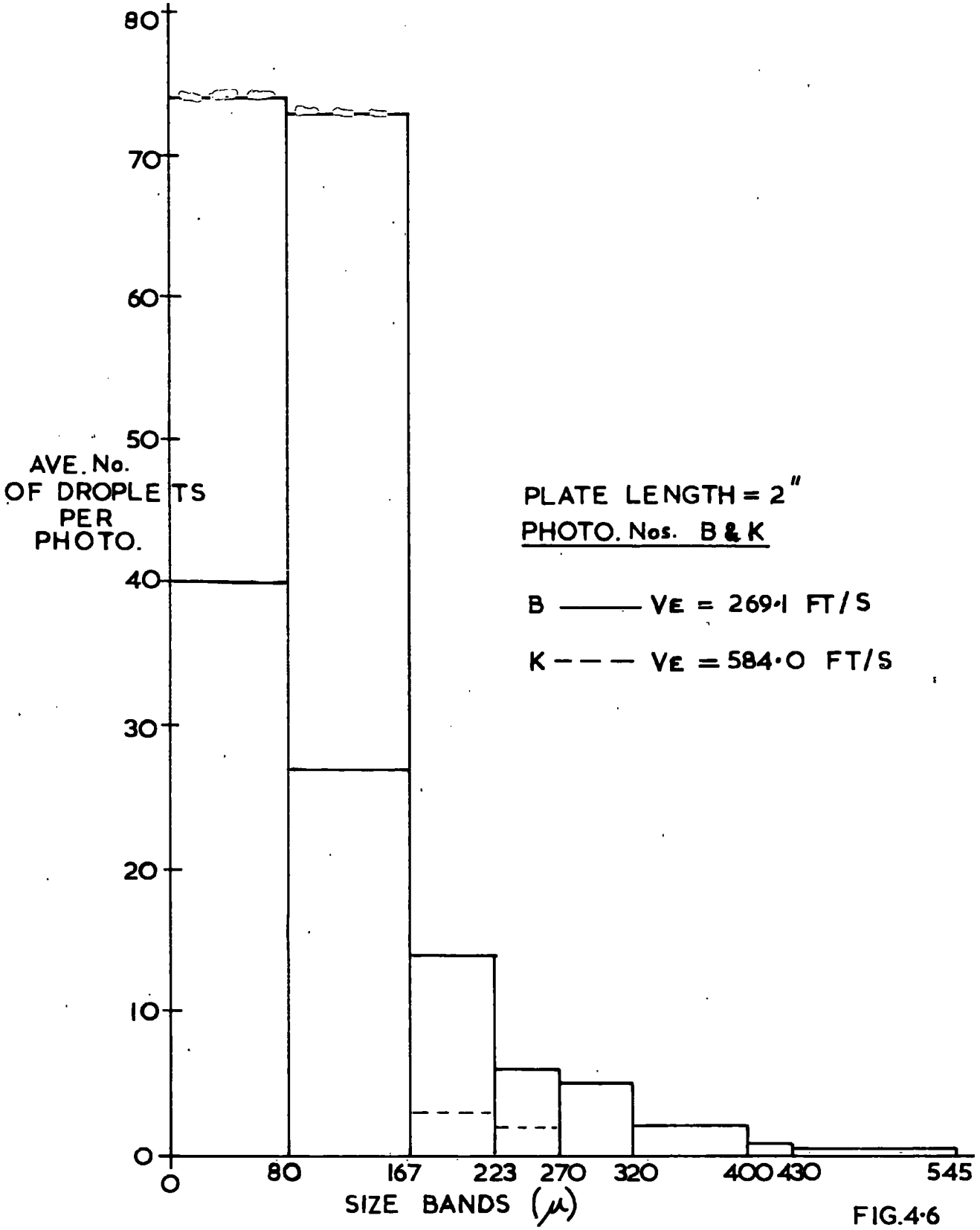

FIG.4·6

VELOCITY TRAVERSE ON ℄ OF 2" PLATE DOWNSTREAM OF TRAILING EDGE

V_W = VELOCITY IN WAKE
V_E = FREE STREAM VELOCITY
P_{T2} = 4·4" T.B.E.

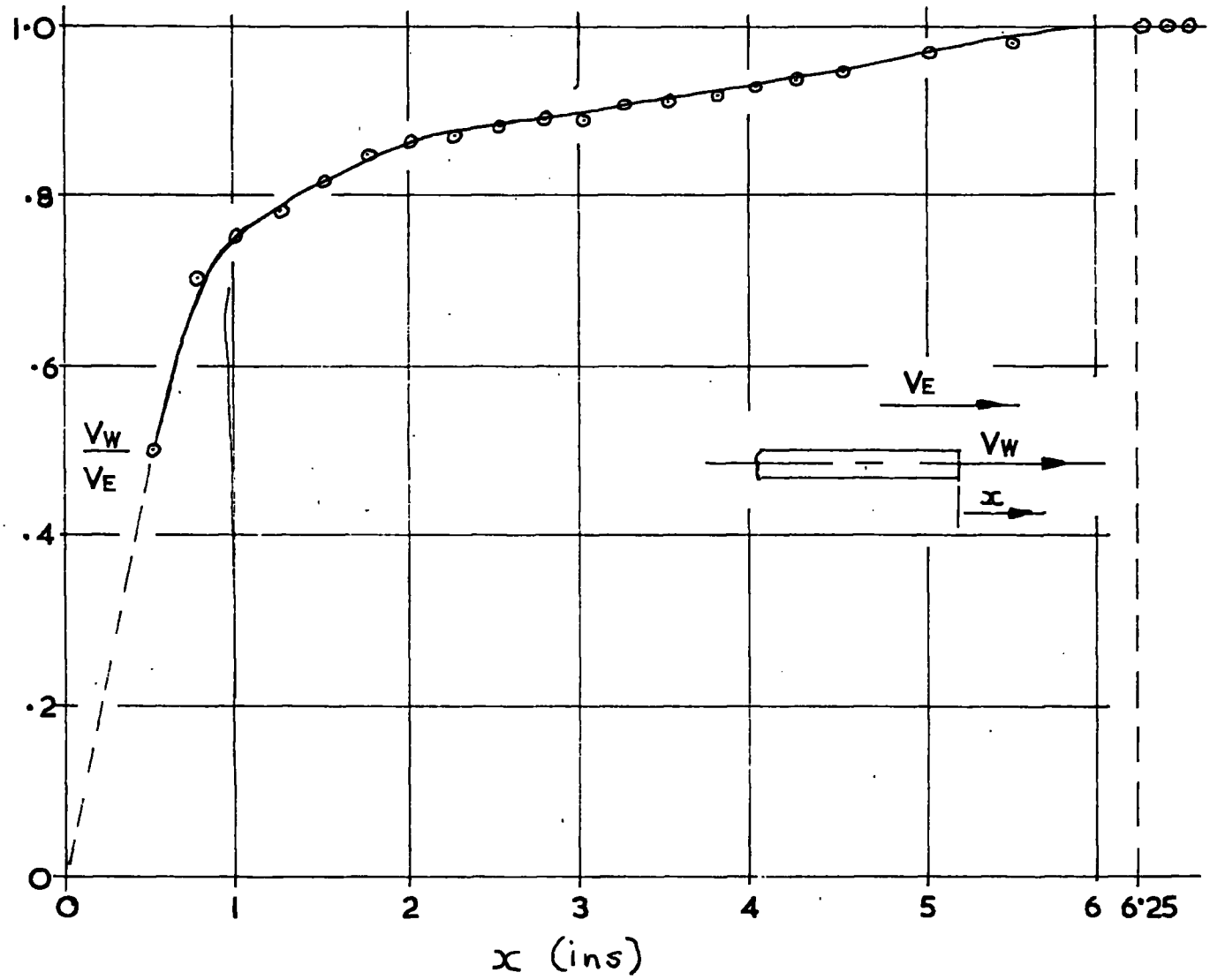

FIG. 4·7

NON DIMENSIONAL PLOT OF TEST RESULTS FOR VARYING PLATE LENGTHS

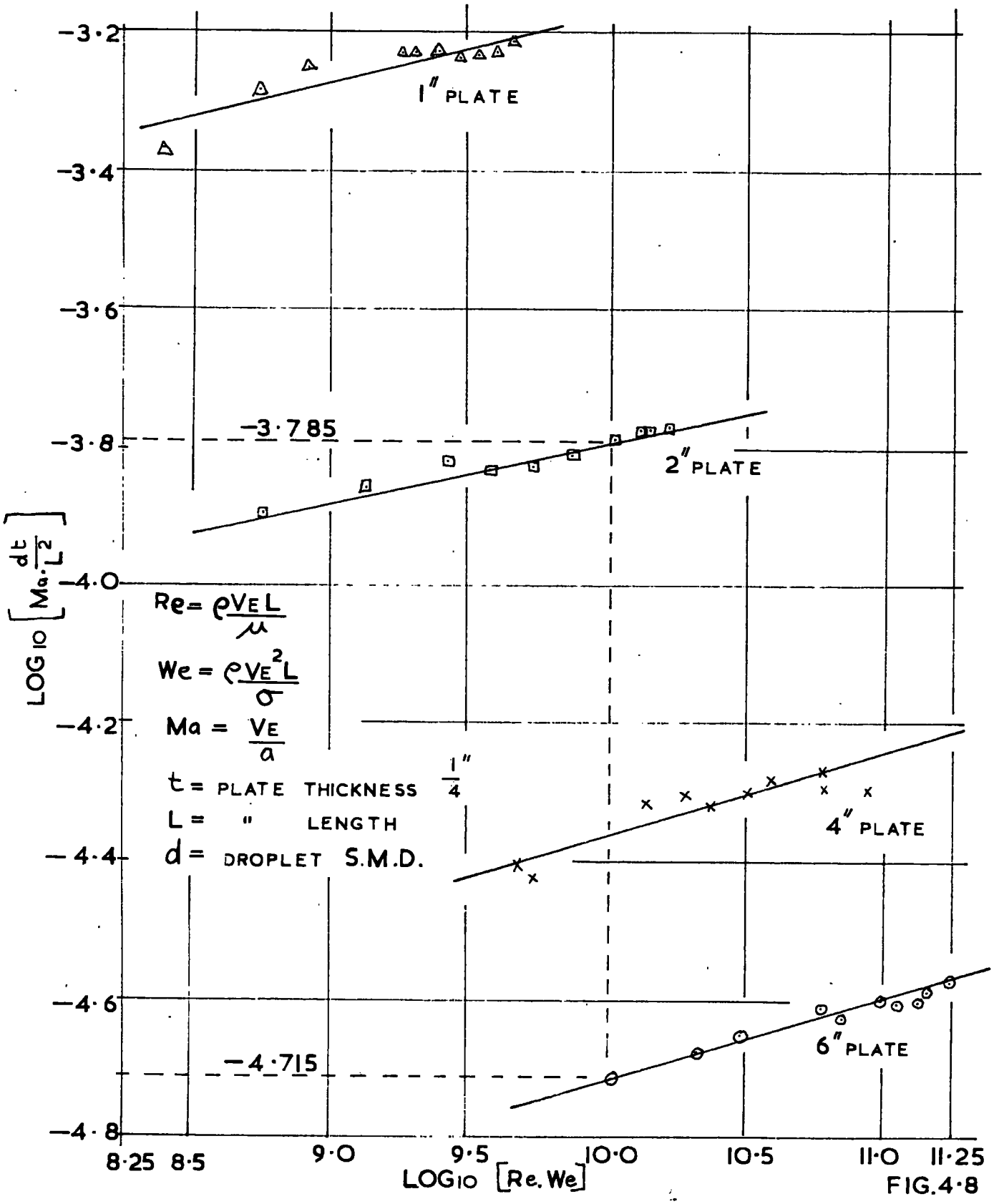

FIG. 4·8

In order to produce a single curve independent of plate length from FIG.4.8, the vertical abscissa was multiplied by $\left(\frac{t}{L}\right)^n$. From FIG.4.8 the two values of LOG_{10} $\left(Ma\ \frac{dt}{L^2}\right)$ recorded for the 2in. and 6in. plate were -3.785 and -4.715 respectively.

$\therefore$ $-4.715 + n \log \left(\frac{t}{L}\right)_6 = -3.785 + n \log \left(\frac{t}{L}\right)_2$

t was constant at $\frac{1}{4}$in.

$\therefore$ $-4.715 + n\ (-1.3799) = -3.785 + n\ (-0.9031)$

$\therefore$ $n = -1.96 \simeq -2.0$

$\therefore$ the vertical abscissa becomes

$$Ma\ \frac{d}{L}\ \frac{t}{L}\left(\frac{t}{L}\right)^{-2} = Ma\ \frac{d}{t}.$$

This is seen to be independent of L. The results were therefore presented as a plot of $Ma\ \frac{d}{t}$ against Re We. as in FIG.4.9.

SINGLE NON DIMENSIONAL PLOT OF TEST RESULTS

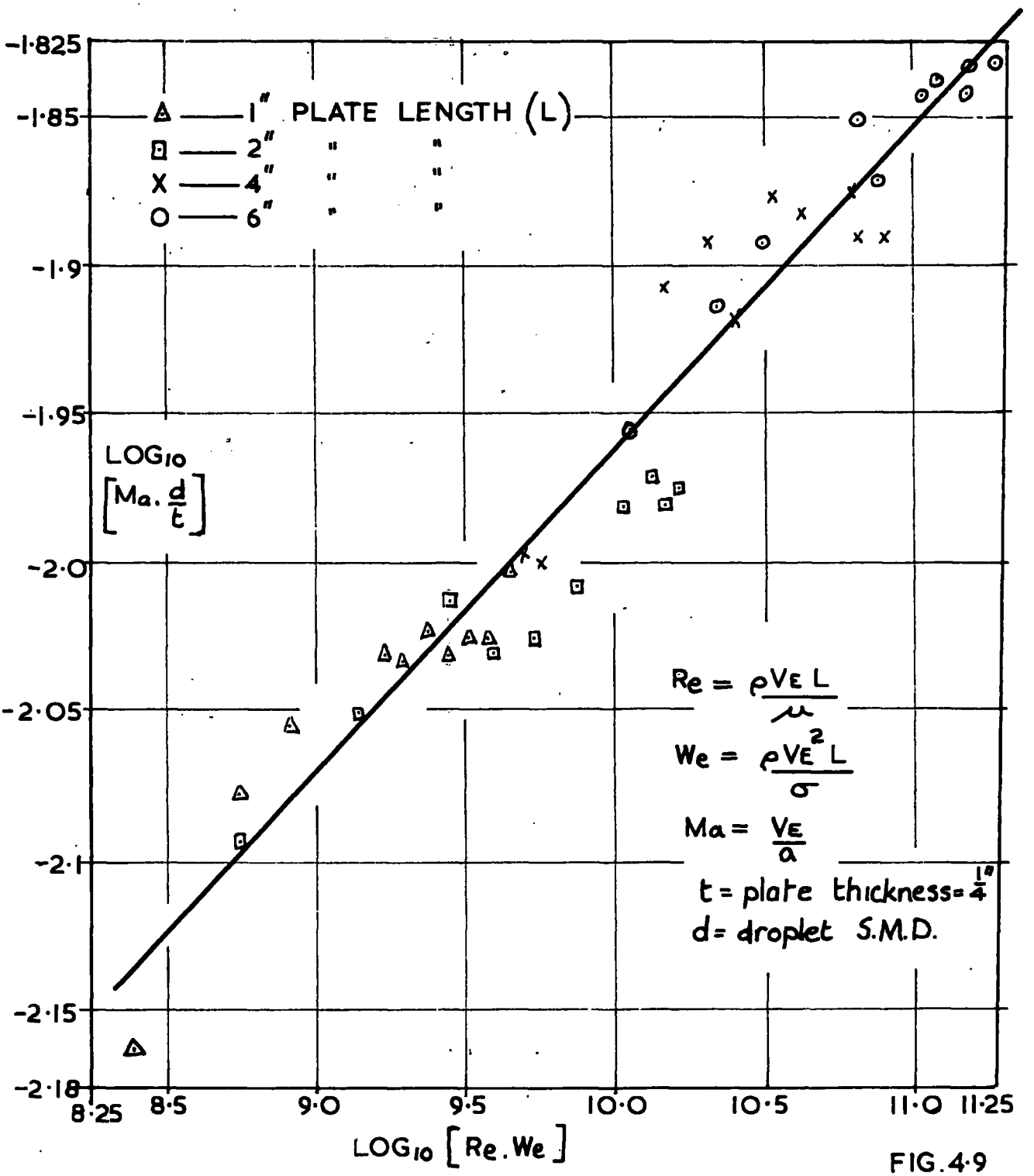

FIG. 4·9

VARIATION OF DROPLET S.M.D. WITH FREE STREAM VELOCITY FOR EACH PLATE LENGTH

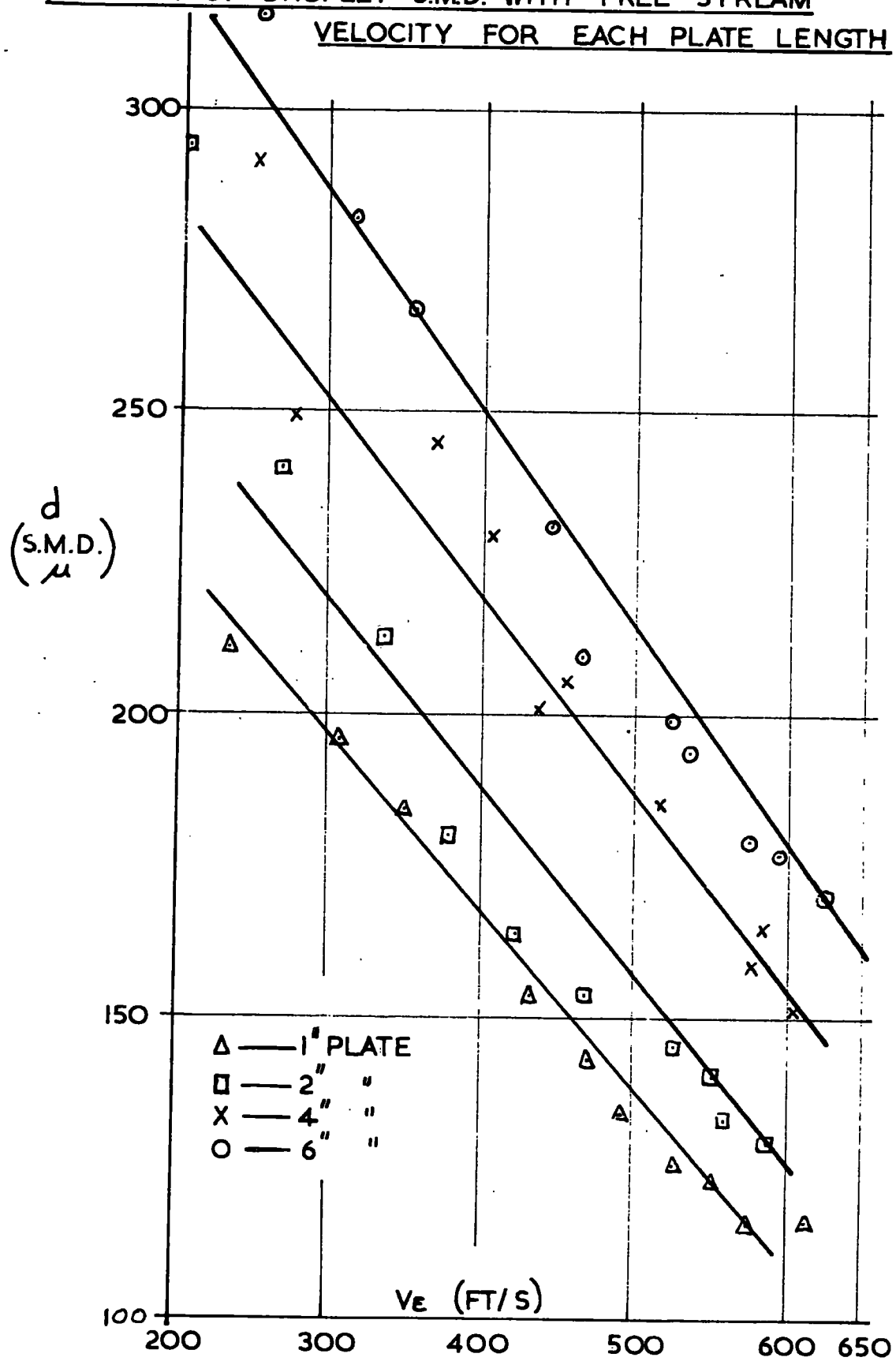

FIG. 4·10

VARIATION OF DROPLET S.M.D. WITH Ve.L

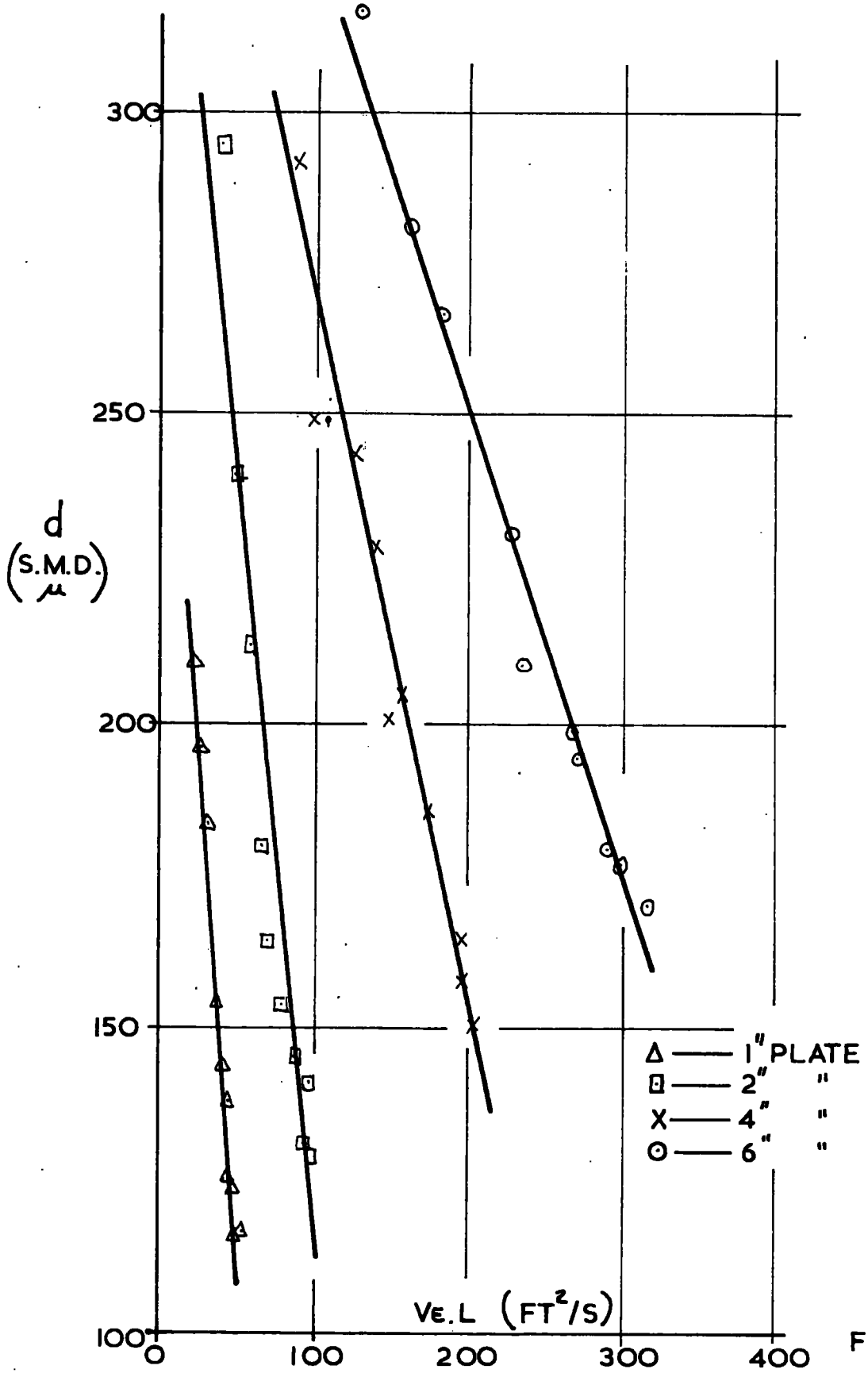

FIG. 4·11

VARIATION OF DROPLET S.M.D. WITH $V_E^2 L$

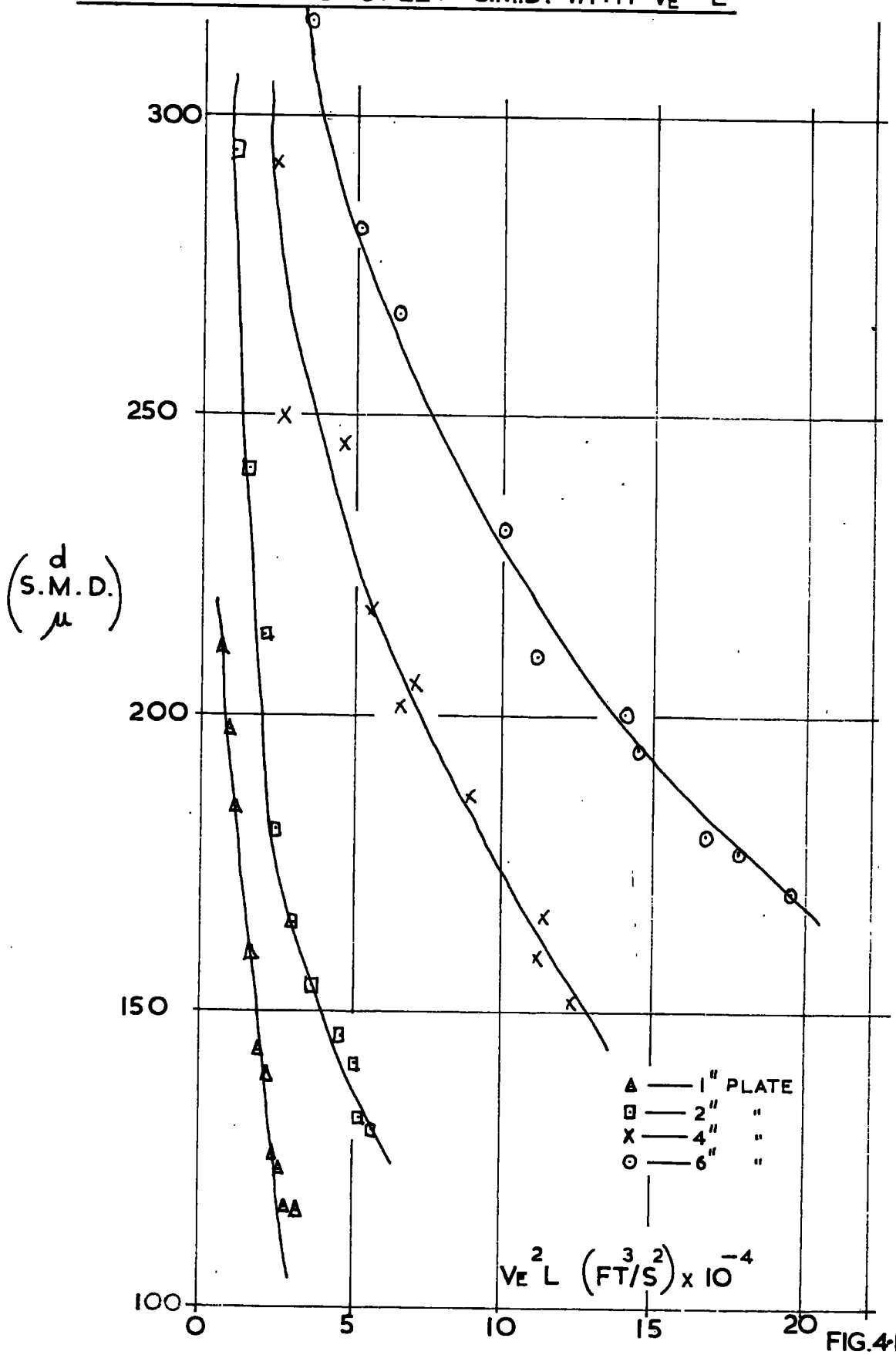

FIG.4·12

5.0 Discussion of Results

The results from the experimental investigation were presented and discussed briefly in chapter 4. In this chapter a deeper analysis of the actual results will be carried out, and where possible, comparison drawn with results from other investigations. There is, however, very little published work on the topic.

Curves have been established which indicate the mean size of droplet produced in varying flow conditions. Use has been made of dimensional analysis, and figure 4.9 enables predictions to be made of droplet size which would be expected from a range of flat plate, fluid flow conditions. The curves for individual plate lengths shown on figure 4.8 exhibit a tendency to level off at high velocity to a constant $Madt/_{L}2$ value where the smaller size droplets tended to dominate.

The substitution of an actual blade profile would improve the conditions at the trailing edge, in as much as the trailing edge of a profiled blade would create a shorter wake length, and would probably generate less turbulence. However, even when allowing for this improvement in trailing edge conditions, the results of the test programme indicate that Gardner (1) in neglecting the effect of the wake zone

on droplet size and velocity has introduced a sizable error. The velocity traverse (Fig. 4.7) indicates a greatly reduced velocity in the immediate trailing edge region. This means that the size of stable droplet is much larger and the approach velocity for a given droplet size is much smaller than Gardner estimated in his paper. The overall effect of the wake on the droplets will be to limit their length of exposure to the free stream velocity when entering the moving row. When taking account of the wake effect therefore the ultimate droplet size will be larger, and although the absolute velocity will be less, it will enter the moving row at an even more accute angle (Fig. 1.1) and would be liable to cause more erosion damage than that estimated for the droplet free from wake effects. It has been shown (1) that the erosion damage varies with the angle of droplet impact up to a maximum for a normal angle of approach. The fact that the ultimate absolute droplet velocity is lower when accounting for wake effects does little to alter the magnitude of impact velocity since it is the blade peripheral speed which is the predominant factor in the resultant droplet impact velocity. Figure 4.6 shows the number of droplets recorded in any size range, and it is evident that over 90% of the droplets were below 250 microns, the larger sizes being relatively few in number. Christie (2) gives a comparable scatter band to those of

figure 4.6 from observations he carries out on a steam turbine last stage. The droplets in question were, however, recorded in the region of the rotor leading edge, that is out of the influence of the stator trailing edge wake. It is, nevertheless, of interest in that his scatter band is of the same proportions.

To form some correlation between the test results and typical conditions existing in a steam turbine, geometric and steam flow parameters existing at the trailing edge of the last stage stator row of a 500 M.W. steam turbine were taken and substituted into the non-dimensional groupings giving a value for the product Re. We of $14.4.10^9$. The Reynolds and Weber numbers were based on blade chord. Reference to figure 4.9 gave the S.M.D. value of droplet formed in the initial breakup period as 94 microns. This value compares favourably with the range quoted by Christie (2) for although it gives a mean value below Christie's, his range was for the droplets as they actually left the trailing edge, and not the mean value calculated over a certain distance downstream from the trailing edge. From the authors observations additional breakup occurs as the droplet accelerates in the immediate trailing edge region. As a general rule one would expect greater additional breakup to occur with the largest droplets. Since deformation is counteracted by surface tension forces, larger droplets will

have less resistance to deformation since their ratio of surface area to mass is lower than that for the smaller droplets. Also Christies photographic recordings were not able to detect droplets less than 50 microns diameter. In the authors test programme it was found that a large percentage of the droplets were in this size range.

The value of mean droplet diameter obtained for the turbine condition from interpolation of figure 4.9 is lower than that obtained from the test programme for the flat plate which had a maximum free stream velocity of 625 ft/s. However the free stream velocity used for the turbine condition was 1150 ft/s, which would suggest that free stream fluid velocity is the main factor in droplet breakup. Figure 4.10 shows that the mean droplet size produced in the immediate trailing edge region varies linearly with free stream velocity over a range of plate lengths. This conclusion is supported by MOORE (3). Thus the lower droplet size range is of the expected form.

The ultimate erosion damage is dependant on the initial droplet formation within the wake zone, and the results thus form a better understanding of wake effects, and a basis for a modified approach to some previous investigations. Since the ratio of wake length to droplet trajectory distance for a typical steam turbine is of the order of 1/3 the author feels that the analysis of the flow of droplets between the stator

trailing edge and the rotor leading edge must be considered as two distinct regimes of flow.

1. The flow within the wake zone itself where this investigation has shown that the initial droplet size is dependant on a number of parameters.

11. The flow prior to the rotor leading edge where the droplet is free from wake effects and theory predicted by Gardner (1) and others can justifiably be applied.

Since a mathematical analysis of the immediate trailing edge region has yet to be formulated, the velocity distribution shown in figure 4.7 could be used and an integrated mean velocity determined. It may then be assumed that the droplet was subjected to this intergrated mean velocity whilst travelling from rest through the wake zone to estimate its velocity when clear of wake influence. Although breakup of the droplet occurs during the acceleration through the wake zone, the greater proportion of the breakup will have occured during the first critical $\frac{3}{4}$ in downstream of the trailing edge. Hence as an approximation the mean droplet size could be assumed to exist throughout the wake and the expression for droplet acceleration applied assuming the droplet to start from rest $\frac{3}{8}$ in from the trailing edge. Thus an expression similar to that used by Gardner (1) could then be used to estimate the condition of the droplet at exit from the wake.

The physical aspects of the water pool transport towards the trailing edge region can be explained as follows. The force Balance between the interfacial tension and aerodynamic forces is the basic concept and the criteria for stability of the water pool. The stream of air flowing over the convex surface of the pool will give rise to a pressure distribution over the surface and in the vicinity of the protruberance a local decrease in pressure corresponding to an increase in velocity will result. The uniform tension on the perturbed interface acts to squeeze the liquid back to the original boundary and hold it in equilibrium. In other words, disturbances in the interface immediately set up an unbalanced opposition of forces. The forces arising from interfacial tension oppose any movement of the interface and attempt to reinstate the original equilibrium, while the aerodynamic forces increase any deviation of the interface and attempt to make the equilibrium unstable. Hence when the resultant aerodynamic force tending to distort the pool is of sufficient magnitude to overcome the ability of the surface tension force to resist distortion there is a resultant movement in the direction of the aerodynamic drag towards the trailing edge. The aerodynamic drag force which is proportional to V_E^2 pulls the water round into the low pressure wake region immediately adjacent to the trailing edge. The parameters governing this

physical process were originally evolved and their justified inclusion discussed in chapter 2. The author's observations of this phenomenan are, in fact, justified and supported by the work of TODD (20). Todd conducted an investigation on a steam turbine with the last stage stator blading modified to a hollow profile form which included slots 0.04 in wide down to the trailing edge. A suction within the blades was applied, this had the effect of drawing off from the trailing edge some of the water which had been formed on it from the previous pool formation on the suction face of the blading. His results indicated a marked reduction in the erosion damage to the following rotor row as compared to the same conditions without the trailing edge slots. This point emphasising that it is the droplets formed from the trailing edge region within the wake that cause the ultimate erosion damage.

The observations of the author on the actual detachment of water once it had been formed along the trailing edge are supported by those of MOORE (3). The action began with the random oscillations of beads of water on the trailing edges. These beads eventually became unstable due to the high degree of turbulence in the immediate trailing edge region. The sheets and ligaments of water formed were broken up by the aerodynamic forces and turbulence of the flow within the immediate trailing edge wake region into a spray of droplets

which were carried downstream under the influence of the initial wake. Due to the very high level of turbulence an equilibrium structure is not to be expected and one cannot mathematically analyse the immediate breakup process in this case except to realize that the boundary layer properties plus trailing edge geometric parameters govern the resultant turbulence level, and hence the resistance of the ligaments to breakup under the action of aerodynamic forces. Whereas the Reynolds, Mach and Weber numbers plus the plate geometric parameters have all been shown to effect the resulting formation and stripping from the trailing edge, the author suggests that it will be the Weber group which governs the further breakup for a given wake condition. This is justified in as much as viscous effects can be ignored due to the high level of turbulence, and low flow velocity in the trailing edge region precludes Mach number effects. In steady state flow the physical processes involved in the breakup of liquid sheets and ligaments are well know but could not be applied to the case in question.

Observations by the author revealed that some of the droplets leaving the pool formed at the plate trailing edge behaved in a similar manner to those described by Smith in discussion with the author (See chapter 1). The size of these droplets

which were produced by the shearing force of the flow on the liquid pool being dependant on the boundary layer properties which vary with flow conditions and plate geometry. They were, however, very small in size and number relative to the main bulk of water flow into the trailing edge wake. Their number was seen to increase very slightly with increasing free stream velocity and decreasing plate length. They were neglected in this investigation since their contribution would have been negligible, and they were under the influence of a different flow regime. In fact, their size and number would have been difficult to record accurately. Analysis of these droplets could be attempted by measurements of the boundary layer profiles and consideration of the resulting shearing forces set up. However, since they were very small relative to the droplets shed into the wake, coupled with the fact that they would be subjected to the main stream velocity and thus rapid acceleration, they are of little interest as regards ultimate erosion damage. TODD (20) supports this by showing that it is the droplets from the wake zone that cause the resulting damage.

The velocity traverse measured in the wake (Fig. 4.7) is compared to Goldsteins theoretical results in (Fig. 5.1). The discrepancy between the curves endorses the author's opinion

that the conditions within the wake zone (for the test curve) were turbulent. In this study the probe situated in the turbulent wake zone would record not only the turbulent velocity component in the x direction, but also a percentage of the velocity components in the y and z directions. Therefore, one would expect the probe in the turbulent wake (which would have a greater interchange of energy with the free stream than a laminar flow) to record a higher velocity than that in the laminar wake for a given probe position, and free stream velocity. This would result in a shorter wake decay length for the turbulent wake under similar conditions. All available experimental work seems to show that the boundary layer on a flat plate becomes turbulent at a value of Reynolds number which depends on the amount of turbulence in the main stream of air outside the layer. In the wind tunnel arrangement used in this project, the air comes to the working section through an abrupt contracting section in which the mean air speed is greatly increased. Allowing also for the relatively abrupt leading and blunt trailing edges, one would expect the transition Reynolds number at the trailing edge to be $< 5.10^5$.

COMPARISON OF THEORETICAL AND EXPERIMENTAL VELOCITY DISTRIBUTION IN WAKE

⊙ — GOLDSTEIN :— THEORETICAL CURVE FOR AN INFINITELY THIN FLAT PLATE (LAMINAR FLOW)

X — EXPERIMENTAL CURVE FOR $\frac{1}{4}''$ THICK PLATE 2" LONG WITH TRAILING EDGE RE OF $2{\cdot}4 \times 10^5$

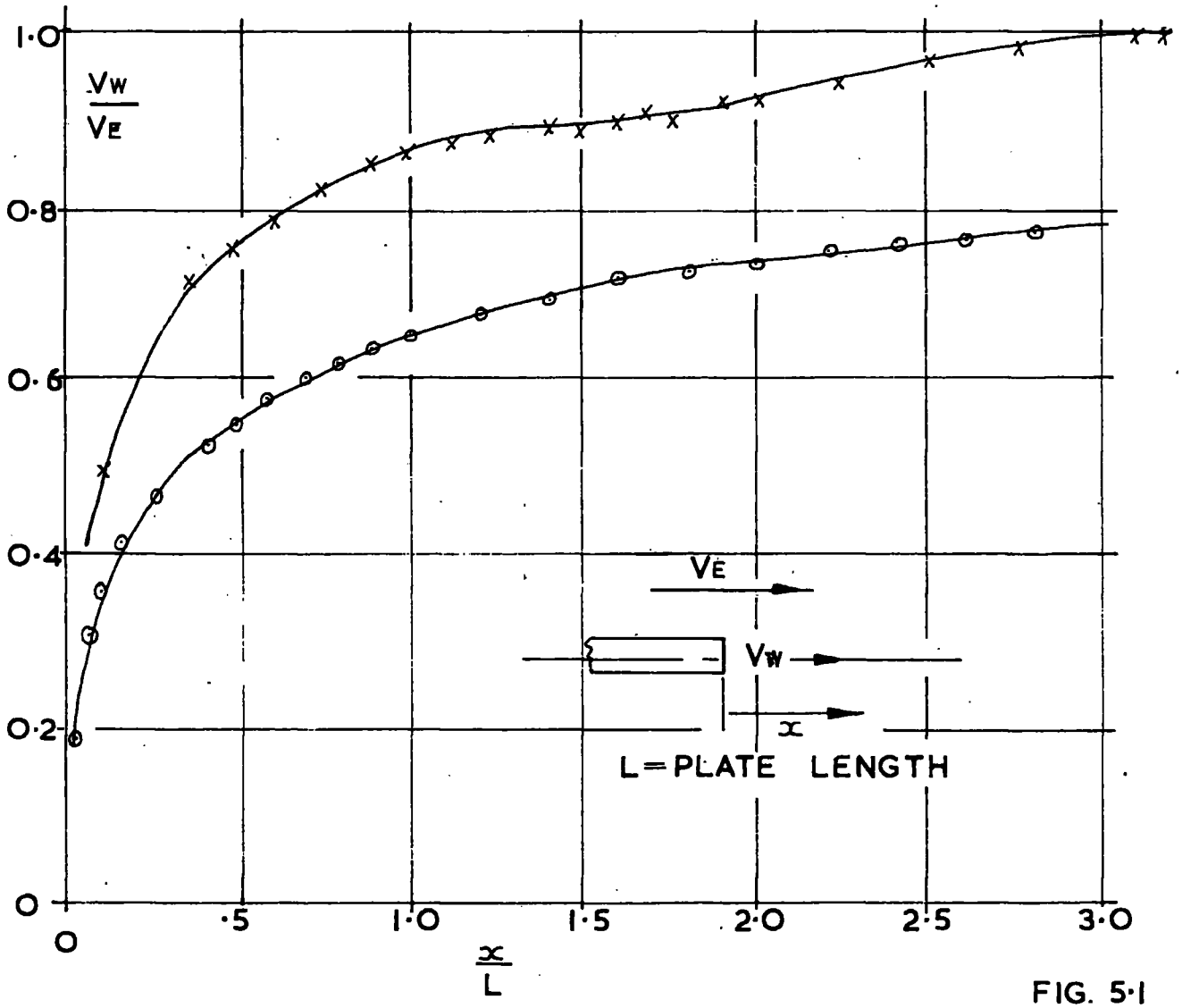

FIG. 5·1

6. Conclusions and Recommendations

The main objective of determining some of the factors governing the formation of water droplets in the wake zone of flat plates, has been accomplished within the limits imposed by the author and outlined in chapter 1. The general conclusions drawn from the project are that

1. The mean droplet size produced in the wake region is primarily a function of free stream velocity and plate length.
2. Visual observation of the stripping action, although conflicting with the investigation from one particular source (5) was seen to be in close agreement with the work of other investigators (3).

It is, however, the author's intention to test plates geometrically similar to those used by Smith in order that some correlation may be obtained. Also, since Moore's work (3) was carried out on blade profiles further geometric similarity will be attempted in this direction.

Owing to the complexity of the overall problem, and the number of variables involved future investigations could be promoted on a number of interesting topics.

1. Use of steam as the working fluid.

There are, however, a number of disadvantages inherent

in using steam instead of air.

a. The test arrangement would have to be closed circuit, returning the steam to a condenser. This would necessitate the use of viewing windows in the tunnel.

b. It is difficult to produce a clear photographic image through windows since they have a tendancy to 'cloud' over when low pressure wet steam is the working fluid.

2. Use of a double flash photographic technique to determine the droplet acceleration within the wake.

Appendices

Appendix 1

Sauter Mean Diameter (S.M.D.)

Two different droplet spectrums may be compared by examining the values of such quantities as the total volume, the total surface area, total radius and total number of droplets. These are given below, the suffix 'o' referring to the fictitious spray composed of equal droplets and suffix '1' denoting the real spray composed of droplets of different sizes.

Total Volume $Vo = \frac{4}{3} \pi No. ro^3$; $V1 = \frac{4}{3} \pi \sum nr^3$

Total Surface Area $Ao = 4 \pi No\ ro^2$; $A1 = 4 \pi \sum nr^2$

Total Radius $Ro = Nor o$; $R1 = \sum nr$

Total Number $No = no$; $N = \sum n$

Here n denotes the number of droplets having radius 'r' in real spray. For the two sprays only two of the four quantities can be equal at the same time, e.g. if it be assumed that $Vo = V1$ and $Ao = A1$. The values of ro and No can be calculated, but it will be seen that if these values of ro and No be substituted in the other equation Ro will not be equal to R1 nor No to N1. Sauter considered the six possible combinations giving two quantities equal for the fictitious and real sprays, and considered that the most convenient was a combination which assumed the same total

surface Ao = Al and the same total volume of droplets Vo = Vl for the two sprays. The value of Γo determined from this condition is called the 'Sauter mean radius' or do = 2ro the 'Sauter mean diameter'. The value of S.M.D. can be readily determined by dividing

$$\frac{Vo}{Ao} = \frac{4/3 \ \pi \ No \ ro^3}{4 \ \pi \ No \ ro^2} = \frac{Ro}{3}$$

$$\therefore do = 6 \frac{Vo}{Ao} = 6 \frac{Vl}{Al}$$

$$\therefore do = 2 \frac{\lesssim nr^3}{\lesssim nr^2}$$

It should be noted that the 'Sauter mean diameter' gives a value which is nearer the size of the bigger droplets of the actual spray, because the volume increases as the 3rd power of the diameter and the surface area as the 2nd, thus the smaller droplets make a relatively smaller contribution to the S.M.D.

Appendix 2

Air Flow Measurement

The following measurements are taken at the upstream tapping position.

P_{s_1} = static pressure

P_{t_1} = total pressure

T_{t_1} = total temperature

P_{s_E} = barometric pressure

Let flow rate at upstream section = W_1 lb/s = $A_1 \omega_1 V_1$

where $V_1 = \sqrt{2ghv}$ (hv = velocity head at 1.) Hence V_E = nozzle exit velocity = $\frac{W_1}{A_E \omega_E}$ ft/s

where A_E = effective exit area of nozzle = 0.0817 ft^2 and ω_E = specific weight of free stream of exit = $2.7 \frac{P_{s_E}}{T_{s_E}}$ lbf/ft^3

and since $T_{t_1} = T_{t_E} = T_{s_E} + \frac{V_E^2}{2gJC_p}$

$$\therefore V_E = \frac{W_1}{A_E 2.7 P_{s_E}} \left[\left(T_{t_1} - \frac{V_E^2}{2gJC_p} \right) + 460 \right]$$

which simplifies to

$$0 = \left[3.805.10^{-4} \frac{W_1}{P_{s_E}} \right] V_E^2 + V_E - 4.57 \frac{W_1}{P_{s_E}} (T_{t_1} + 460)$$

This quadratic was solved for values of V_E on substituting the measured values of W_1, P_{s_E} and T_{t_1}.

Appendix 3

Droplet Sampling Techniques

There are two basic methods available to determine the water droplet sizes in the air flow downstream of the plate trailing edge.

1. Direct Physical Sampling

This is usually accomplished by having drops impinge on microscope slides in the spray. The captured sample can then be analyzed leisurely for number and size of droplets. This procedure is untrustworthy because it is questionable if the sample analysed is representative of original droplet formation. Also if the slide is moved rapidly across the spray it can cause splitting of the larger droplets. The work of Langmuir and Blodgett (16) indicates that any impingement process discriminates against capturing small droplets. May (17) carried out a complete calibration, detecting and measuring airborne droplets whereby a permanent impression was made by the droplets striking a layer of magnesium oxide, smoked on a glass slide and measuring the impressions microscopically. For a range of droplet size 10 - 200 microns he found the ratio of drop size to impression size to be constant at 0.85. The method fails, however, for droplets below 10 microns where the droplets tend to bounce.

For recent developments in physical sampling of water droplets, the reader is referred to reference (18).

2. Indirect Methods of Droplet Measurement

The indirect methods can be subdivided into the following groups

a. Photometric:- based on a decrease in intensity of a beam of light passing through a spray Sauter found the light lost in passing through the spray proportional to the droplet diameter. The interpretation of the results is, however, extremely difficult when the droplets of the spray are not in a very narrow range of sizes. It is also impossible to determine number of droplets and individual sizes.

b. Electric:- based on assumption that electrical capacity of a droplet is proportional to the diameter. Hence by charging droplet to a given potential and measuring the total amount of electricity in droplet, the capacity of the droplet can be determined. This method is valid only if it is assumed that the droplets are not effected by induction from adjacent charged conductors.

c. Kinetic:- from a measurement of momentum of the spray the mean droplet size can be calculated. This method would disturb the flow pattern.

d. Thermal:- based on rate of droplet evaporation. The rate of evaporation would be very small and therefore difficult to analyse accurately.

e. Photographic:- there are two ways of photographing high speed phenomena

1. high speed cine-camera with a constant illumination.
2. illuminating by a very short and intense flash while the camera shutter is open.

This latter method upon which modern research workers have come to depend on a great deal is the method employed in this research project. A more detailed account of methods of droplet measurement can be found in reference (19).

Since a photographic method does not require any objects in the stream, the results are free from disturbances of the flow pattern. The interpretation is, however, difficult when the drops are not in a narrow band. The recording of an event occurring in a fluid at very high velocity can only be achieved with a very brief exposure time. In a high velocity flow a droplet may be travelling up to 1000 ft/s., thus considering a droplet 30 microns diameter in order to produce an image so that the blur in the direction of motion is less than say $\frac{1}{2}$ diameter, the

duration of the illuminating flash must be about 0.05 microsec. This effect could, in fact, be utilised to determine the velocity of the droplets.

Appendix 4

Electric Spark in Air

The electric spark in air gives a brief duration. The intensity of light produced in an open spark gap is a function of the energy dissipated in the gap and the volume in which this energy is dissipated. The portion of the available energy in the capacitors that goes into the gap depends upon the ratio of gap resistance to total circuit resistance. The time energy characteristic of a capacitor discharge in air is oscillatory, the time intervals of the oscillations being considerably reduced by employing specially designed capacitors and by connecting the electrodes directly across the terminals in order to keep the inductance in the leads as small as possible. For exposures of the shortest duration it is necessary to keep the electrical capacity low and voltage high. At the same time it is necessary to employ the smallest possible light source at the maximum practical distance to obtain near parallel light. The problems common to all capacitor discharge spark supplies are those of finding a reliable means of initiating the discharge and maintaining a high impedence in the gap to provide a rapid rise in light intensity with efficient energy conversion into useful light output.

Appendix 5.

Calibration of Air Flow Rate

From the total head traverse FIG.App.(5.1) the mean velocity head at exit was found to be 20.0 in TBE.

Atmospheric pressure = 14.85 p.s.i.

exit gas temperature = $75^{\circ}F$

$\therefore \omega_E = 0.075$ lbf/ft^3

Effective exit area = 0.0817 ft^2

$\therefore$ velocity head in ft. of air $= \frac{20.\ 62.4\ 2.95}{12 \quad .075}$

$= 4060$ ft.

$\therefore 4060 = \frac{V_E^2}{2g} \left[1 + \frac{Ma^2}{4} \right]$

allowing for compressibility and $Ma = \frac{V_E}{\sqrt{\gamma g R T_E}}$ hence

$V_E = 496$ ft/s.

$\therefore$ Exit flow rate $= 496.\ .075\ \ .0817$

$= \underline{3.04 \text{ lb/s.}}$

The flow rate at the upstream position assuming incompressible flow was found to be 2.99 lb/s.

TOTAL HEAD TRAVERSE $\frac{3}{4}$ IN. FROM LEADING EDGE OF 2 IN PLATE $\frac{1}{16}$ IN ABOVE SURFACE

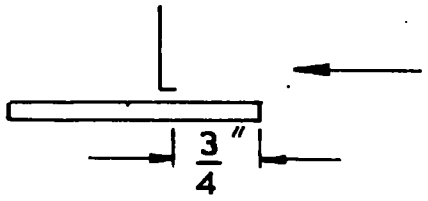

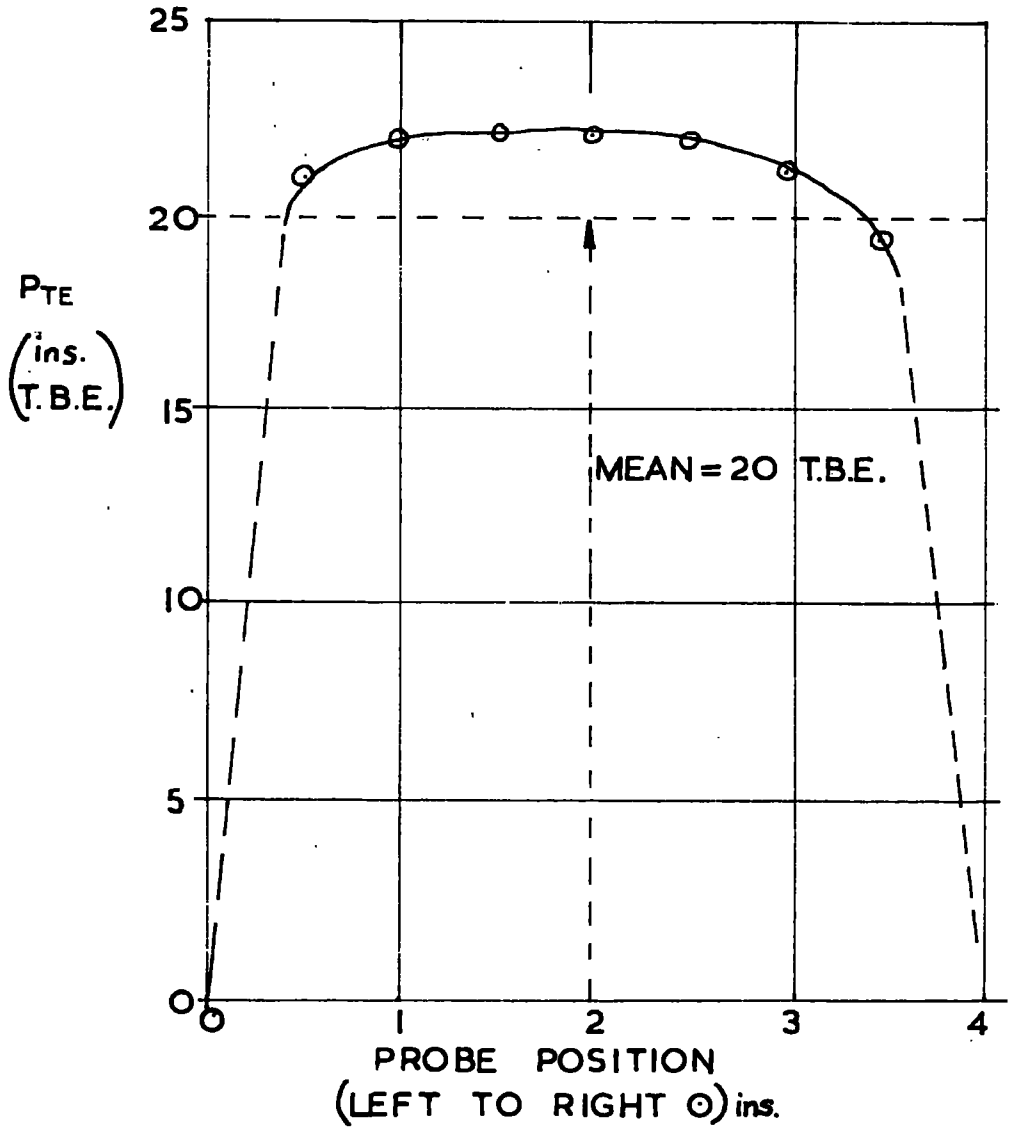

FIG. $A_{pp}5{\cdot}1$

Appendix 6

FLOW PARAMETERS FOR VARYING PLATE LENGTHS

Test No.	Photo Ref.No.	Ma	Re x 10^{-5}	We x 10^{-3}	Free Stream Velocity V ft/s	Plate Length L (inches)
D1	j	0.207	1.16	2.082	235	
D1	k	.27	1.5	3.54	307.6	
D1	l	.306	1.7	4.56	350	
D2	m	.387	2.21	7.3	431	
D2	n	.412	2.29	8.26	470	1
D3	o	.435	2.45	9.23	491	
D3	p	.466	2.585	10.65	529	
D3	q	.485	2.682	11.63	551	
D4	r	.51	2.86	12.48	576	
D5	s	.54	2.988	13.9	613	
A6	M	0.174	1.88	2.9	200.5	
A1	B	.234	2.5	5.25	269.1	
A1	C	.289	3.15	8.05	333	
A1	D	.328	3.5	10.31	378.2	
A2	E	.365	3.98	12.95	420	2
A3	G	.404	4.43	16.02	464.5	
A2	F	.457	4.95	20.2	526	
A3	H	.484	5.41	23.4	552	
A4	J	.495	5.62	23.75	556	
A5	K	.52	5.92	26.15	584	
B1	M	0.219	4.9	9.26	250	
B4	e	.243	5.34	10.4	274	
B1	N	.322	7.03	19.75	367	
B4	f	.356	7.9	24.4	405	
B1	O	.384	8.34	28.31	440	
B5	g	.412	9.5	33.0	454	
B2	P	.45	9.8	39.4	517	4
B2	Q	.511	11.4	51.4	583	
B6	h	.515	11.66	51.7	578	
B3	R	.541	12.85	58.4	605	

Contd.....

Test No.	Photo Ref.No.	Ma	Re x 10^{-5}	We x 10^{-3}	Free Stream Velocity V ft/s	Plate Length L (inches)
C1	S	0.222	7.48	14.41	252	6
C2	a	.275	9.3	22.1	312	
C1	T	.307	10.36	27.7	351	
C1	U	.389	12.91	44.3	444	
C2	b	.408	13.8	48.7	464	
C1	V	.46	15.5	62.3	525	
C3	c	.478	16.0	65.2	538	
C1	W	.508	17.24	76.0	577	
C4	d	.525	17.2	78.0	593	
C1	x	.55	18.7	88.5	624	

Water flow rate to plate constant at $0.246.10^{-2}$ lb/s.

Pool depth constant at 0.005 in.

Plate thickness constant at 0.25 in.

TABLE 6.1

PHOTOGRAPHIC RECORDINGS FOR 1 INCH PLATE

Test No.	Photo Ref. No.	Largest Droplet Record-ed (Mic-rons)	Smallest Droplet Record-ed (Mic-rons)	Number of Drop-lets Record-ed	S.M.D. (Mic-rons)	Mean S.M.D. (Mic-rons)
D1	j1 j2 j3	415 415 360	<80	98 144 136	227 205 200	211
D1	k1 k2 k3	415 487 415	"	158 178 126	200 206 184	197
D1	l1 l2 l3	360 360 415	"	122 157 209	180 177 195	184
D2	m1 m2 m3	360 360 415	"	186 121 336	147 150 165	154
D2	n1 n2 n3	360 360 295	"	160 344 177	148 141 142	143
D3	01 02 03	246 295 246	"	163 177 196	138 148 131	139
D3	p1 p2 p3	246 246 295	"	182 215 431	128 126 123	126
D3	q1 q2 q3	246 246 246	"	282 210 226	123 125 121	123

Contd.....

Test No.	Photo Ref. No.	Largest Droplet Record-ed (Mic-rons)	Smallest Droplet Record-ed (Mic-rons)	Number of Drop-lets Record-ed	S.M.D. (Mic-rons)	Mean S.M.D. (Mic-rons)
D4	r1 r2 r3	246 246 246	80	457 478 371	114 118 119	117
D5	s1 s2 s3	246 246 246	"	344 304 458	117 119 116	117

TABLE 6.2

PHOTOGRAPHIC RECORDINGS FOR 2 INCH PLATE

Test No.	Photo Ref. No.	Largest Droplet Recorded (Microns)	Smallest Droplet Recorded (Microns)	Number of Droplets Recorded	S.M.D. (Microns)	Mean S.M.D. (Microns)
A6	M1 M2 M3	415 415 487	<80	110 55 58	231 370 281	294
A1	B1 B2 B3	487 360 360	"	134 100 52	252 244 227	241
A1	C1 C2 C3	360 415 360	"	100 138 123	206 219 215	213
A1	D1 D2 D3	295 295 246	"	114 112 129	181 185 174	180
A2	E1 E2 E3	360 295 295	"	145 120 117	173 157 161	164
A3	G1 G2 G3	295 360 295	"	142 160 162	151 154 148	154
A2	F1 F2 F3	246 295 295	"	133 135 147	142 146 149	146
A3	H1 H2 H3	246 295 246	"	146 135 153	135 144 143	141

Contd.....

Test No.	Photo Ref. No.	Largest Droplet Recorded (Microns)	Smallest Droplet Recorded (Microns)	Number of Droplets Recorded	S.M.D. (Microns	Mean S.M.D. (Microns)
A4	J1 J2 J3	246 246 246	< 80	213 188 165	130 134 133	132
A5	K1 K2 K3	246 246 246	"	154 144 159	131 120 136	129

TABLE 6.3

PHOTOGRAPHIC RECORDINGS FOR 4 INCH PLATE

Test No.	Photo Ref. No.	Largest Droplet Recorded (Microns)	Smallest Droplet Recorded (Microns)	Number of Droplets Recorded	S.M.D. (Microns)	Mean S.M.D. (Microns)
B1	M1 M2 M3	487 487 487	<80	160 85 89	285.2 295 297	292
B4	e1 e2 e3	487 487 594	"	252 142 254	255 264 227	249
B1	N1 N2 N3	487 415 487	"	114 117 101	247 238 248	244
B4	f1 f2 f3	415 594 415	"	159 138 118	225 254 210	229
B1	O1 O2 O3	415 415 360	"	136 108 156	193.6 219 189	200.5
B5	g1 g2 g3	487 487 360	"	238 163 149	193 232 190	205
B2	P1 P2 P3	295 415 360	"	102 202 170	182 185 186.5	184.5
B2	Q1 Q2 Q3	295 360 360	"	136 125 136	162 161.5 172	164.6

Contd.....

Test No.	Photo Ref. No.	Largest Droplet Recorded (Microns)	Smallest Droplet Recorded (Microns)	Number of Droplets Recorded	S.M.D. (Microns)	Mean S.M.D. (Microns)
B6	h1 h2 h3	295 360 295	<80	142 201 164	149 165 162	158
B3	R1 R2 R3	295 295 295	"	179 192 251	142 156 154	151

TABLE 6.4

PHOTOGRAPHIC RECORDINGS FOR 6 INCH PLATE

Test No.	Photo Ref. No.	Largest Droplet Recorded (Microns)	Smallest Droplet Recorded (Microns)	Number of Droplets Recorded	S.M.D. (Microns)	Mean S.M.D. (Microns)
C1	S1 S2 S3	594 487 594	<80	138 100 181	322 307 323	317
C2	A1 A2 A3	487 487 594	"	72 208 78	278 277 292	282
C1	T1 T2 T3	594 487 594	"	124 130 168	271 246 286	267
C1	U1 U2 U3	487 487 487	"	208 160 179	220 237 236	231
C2	b1 b2 b3	415 415 415	"	133 139 76	208 216 204	209
C1	V1 V2 V3	415 487 487	"	179 255 243	215 201 182	199
C3	C1 C2 C3	487 415 415	"	182 145 96	190 180 214	194
C1	W1 W2 W3	360 360 415	"	251 248 256	165 181 190	179

Contd.....

Test No.	Photo Ref. No.	Largest Droplet Recorded (Microns)	Smallest Droplet Recorded (Microns)	Number of Droplets Recorded	S.M.D. (Microns)	Mean S.M.D. (Microns)
C4	d1 d2 d3	415 360 415	<80	165 191 161	174 172 185	177
C1	x1 x2 x3	360 487 360	"	329 239 317	161.5 179 170	170

TABLE 6.5

Nomenclature

Al tunnel cross sectional area at upstream tapping position.

A_E effective nozzle exit area.

a speed of sound in exit air stream $= \sqrt{\gamma g R T_{sE}}$

d droplet diameter.

K_E bulk modules of free stream air.

hv velocity head.

L plate length.

Ma mach number $= \frac{V_E}{a}$

Psl static pressure at upstream position.

P_{sE} barometric pressure.

Ptl total pressure at upstream position.

P_{tE} total pressure at nozzle exit.

R gas constant.

Re reynolds number $= \frac{\rho_E V_E L}{\mu_E}$

r droplet radii

T_{sE} static temperature of air stream at nozzle exit.

Ttl total temperature of air stream at upstream position.

T_{tE} total temperature of air stream at nozzle exit.

t plate thickness.

Vl air velocity at upstream position.

V_E free stream air velocity at nozzle exit.

V_w air flow velocity within plate trailing edge wake.

W_1 air flow rate at upstream position.

W_E weber number $= \frac{\rho_E V_E^2 L}{\sigma}$ *

w_1 specific weight of air at upstream position.

w_E specific weight of free air stream at nozzle exit.

γ isentropic index.

μ_E viscosity of free air stream at nozzle exit.

ρ_E free stream air density at nozzle exit.

σ surface tension of water.

*this definition of weber number is not of the standard form, the justification for this is explained in chapter 2.

References

1. Gardner, G.C. 'Events leading to erosion in the steam turbine'.
PROC. 1. MECH. ENG. 1963-64.
VOL. 178 PART 1 No.23.

2. Christie, D.G. 'The formation of water drops which cause turbine blade erosion' paper 4. Thermodynamics and Fluid mechanics convention Liverpool 1966.

3. Moore, M.J. 'Research at C.E.R.L. on turbine blade erosion' paper 5. Thermodynamics and Fluid mechanics convention Bristol 1968.

4. Law, J.O. TRANS. A.M. GEOPHYS. UNION 194022 PT.3 709.

5. Smith, A, Kent, R.P. and Armstrong, R.L. 'Erosion of steam turbine blade shield materials'.
ASTM STP 408 American Society for testing and materials 1967 P.125.

6. Lane, W.R. 'Shatter of drops in streams of air'
IND. ENG. CHEM. VOL. 43. June 1951.

7. Lapple, C.E. and Shepherd, C.B. 'Calculation of particle trajectories'
IND. ENG. CHEM. 1940 32, 605.

8. Soderberg, C.R. 'The importance of moisture in steam turbines' The Electric Journal, July 1934.

9. Schlichting, H. 'Boundary Layer Theory'.
London. Pergamon Press.

10. Goldstein, S. 'Modern Developments in fluid dynamics'
Oxford Press.

11. Kline, S.J. 'Some remarks on turbulent shear flows' nominated lecture. Thermodynamics and Fluid mechanics convention. Liverpool 1966.

12. Goldstein, S. 'Flow of a viscous fluid behind a solid body'.
PROC. of Royal Soc. A 142 (1933) 545 - 560.

13. Fage, A. and Fakner. PROC. of Royal Soc. A 142 (1933) 560 - 562.

14. Buckingham, E. 'Model experiments and the form of empirical equations'.
TRANS. A.S.M.E. VOL. 37 PP 263 - 296 1915.

15. Taylor, J.F. 'Isothermal free jets of air mixing with air'. CHEM. ENG. PROG. VOL. 47 No.4. P 175.

16. Langmuir, I. and Bladgett, K.B. 'A mathematical investigation of water droplet trajectories' U.S.A.A.F. Tech. rept. 5418 1946.

17. May, K.R. 'The measurement of airborne droplets by the magnesium oxide method' JOUR. SCIENTIFIC INSTT VOL. 27. May 1950.

18. Ryley, D.J. and Fallon, J.B. 'Size sampling of steam-borne water droplets' paper 25. Thermodynamics and Fluid mechanics convention Liverpool 1966.

19. Griffen, E. and Muraszew, A. 'The atomization of liquid fuels'. Chapman and Hall.

20. Todd, K.W. and Gregory, B. 'An Experiment on erosion control using a 60 M.W. steam turbine' Paper 31 Thermodynamics and Fluid Mechanics Convention Bristol 1968.

Figures and Illustrations

Figures and illustrations are given at the end of each chapter to which they relate.

Acknowledgements

The author would like to express his sincere thanks to Professor R. Hoyle of the Department of Engineering and Science, University of Durham for initially providing the opportunity to submit this thesis, and thereafter for his valued guidance.

Thanks are also due to the authorities of Sunderland Polytechnic and, in particular, to the Departmental Head of Mechanical Engineering. Without their patronage the project could not have commenced.